

A previously overlooked, highly diverse early Pleistocene elasmobranch assemblage from southern Taiwan (#73574)

1

First revision

Guidance from your Editor

Please submit by **11 Aug 2022** for the benefit of the authors .



Structure and Criteria

Please read the 'Structure and Criteria' page for general guidance.



Raw data check

Review the raw data.



Image check

Check that figures and images have not been inappropriately manipulated.

Privacy reminder: If uploading an annotated PDF, remove identifiable information to remain anonymous.

Files

Download and review all files from the [materials page](#).

1 Tracked changes manuscript(s)
1 Rebuttal letter(s)
21 Figure file(s)
4 Table file(s)



Structure your review

The review form is divided into 5 sections. Please consider these when composing your review:

- 1. BASIC REPORTING**
- 2. EXPERIMENTAL DESIGN**
- 3. VALIDITY OF THE FINDINGS**
4. General comments
5. Confidential notes to the editor

You can also annotate this PDF and upload it as part of your review

When ready [submit online](#).

Editorial Criteria

Use these criteria points to structure your review. The full detailed editorial criteria is on your [guidance page](#).

BASIC REPORTING

- Clear, unambiguous, professional English language used throughout.
- Intro & background to show context. Literature well referenced & relevant.
- Structure conforms to [PeerJ standards](#), discipline norm, or improved for clarity.
- Figures are relevant, high quality, well labelled & described.
- Raw data supplied (see [PeerJ policy](#)).

EXPERIMENTAL DESIGN

- Original primary research within [Scope of the journal](#).
- Research question well defined, relevant & meaningful. It is stated how the research fills an identified knowledge gap.
- Rigorous investigation performed to a high technical & ethical standard.
- Methods described with sufficient detail & information to replicate.

VALIDITY OF THE FINDINGS

- Impact and novelty not assessed. *Meaningful* replication encouraged where rationale & benefit to literature is clearly stated.
- All underlying data have been provided; they are robust, statistically sound, & controlled.

- Conclusions are well stated, linked to original research question & limited to supporting results.

Standout reviewing tips

3



The best reviewers use these techniques

Tip

Support criticisms with evidence from the text or from other sources

Give specific suggestions on how to improve the manuscript

Comment on language and grammar issues

Organize by importance of the issues, and number your points

Please provide constructive criticism, and avoid personal opinions

Comment on strengths (as well as weaknesses) of the manuscript

Example

Smith et al (J of Methodology, 2005, V3, pp 123) have shown that the analysis you use in Lines 241-250 is not the most appropriate for this situation. Please explain why you used this method.

Your introduction needs more detail. I suggest that you improve the description at lines 57- 86 to provide more justification for your study (specifically, you should expand upon the knowledge gap being filled).

The English language should be improved to ensure that an international audience can clearly understand your text. Some examples where the language could be improved include lines 23, 77, 121, 128 - the current phrasing makes comprehension difficult. I suggest you have a colleague who is proficient in English and familiar with the subject matter review your manuscript, or contact a professional editing service.

1. Your most important issue
2. The next most important item
3. ...
4. The least important points

I thank you for providing the raw data, however your supplemental files need more descriptive metadata identifiers to be useful to future readers. Although your results are compelling, the data analysis should be improved in the following ways: AA, BB, CC

I commend the authors for their extensive data set, compiled over many years of detailed fieldwork. In addition, the manuscript is clearly written in professional, unambiguous language. If there is a weakness, it is in the statistical analysis (as I have noted above) which should be improved upon before Acceptance.

A previously overlooked, highly diverse early Pleistocene elasmobranch assemblage from southern Taiwan

Chia-Yen Lin Equal first author, 1, **Chien-Hsiang Lin** Corresp., Equal first author, 1, **Kenshu Shimada** 2, 3

¹ Biodiversity Research Center, Academia Sinica, Taipei, Taiwan

² Department of Environmental Science and Studies and Department of Biological Sciences, DePaul University, Chicago, Illinois, The United States of America

³ Sternberg Museum of Natural History, Fort Hays State University, Hays, Kansas, The United States of America

Corresponding Author: Chien-Hsiang Lin
Email address: chlin.otolith@gmail.com

The Niubu fossil locality in Chiayi County, southern Taiwan is best known for its rich early Pleistocene marine fossils that provide insights into the poorly understood past diversity in the area. The elasmobranch teeth at this locality have been collected for decades by the locals, but are not formally described and have received little attention. Here, we described three museum collections of elasmobranch teeth ($n = 697$) from the Liuchungchi Formation (1.90–1.35 Ma) sampled at Niubu locality, with an aim of constructing a more comprehensive view of the past fish fauna in the subtropical West Pacific. The assemblage is composed of 20 taxa belonging to 9 families and is dominated by *Carcharhinus* and *Carcharodon*. The occurrence of *Hemipristis serra* is of particular importance because it is the first Pleistocene record in the area. We highlight high numbers of large *Carcharodon carcharias* in our sample exceeding 4 m, along with the diverse fossil elasmobranchs, suggesting that a once rich and thriving marine ecosystem in an inshore to offshore shallow-water environment during the early Pleistocene in Taiwan.

1 **A previously overlooked, highly diverse early**
2 **Pleistocene elasmobranch assemblage from southern**
3 **Taiwan**

4

5

6 Chia-Yen Lin^{1, #}, Chien-Hsiang Lin^{1, #}, Kenshu Shimada^{2,3}

7

8

9 ¹ Biodiversity Research Center, Academia Sinica, Taipei, Taiwan

10 ² Department of Environmental Science and Studies and Department of Biological Sciences,
11 DePaul University, Chicago, Illinois, USA

12 ³ Sternberg Museum of Natural History, Fort Hays State University, Hays, Kansas, USA

13 [#] Equal first author

14

15 Corresponding Author:

16 Chien-Hsiang Lin¹

17 Biodiversity Research Center, Academia Sinica, Taipei, Taiwan

18 Email address: chlin.otolith@gmail.com

19

20 **Abstract**

21 The Niubu fossil locality in Chiayi County, southern Taiwan is best known for its rich early
22 Pleistocene marine fossils that provide insights into the poorly understood past diversity in the
23 area. The elasmobranch teeth at this locality have been collected for decades by the locals, but
24 are not formally described and have received little attention. Here, we described three museum
25 collections of elasmobranch teeth (n = 697) from the Liuchungchi Formation (1.90–1.35 Ma)
26 sampled at Niubu locality, with an aim of constructing a more comprehensive view of the past
27 fish fauna in the subtropical West Pacific. The assemblage is composed of 20 taxa belonging to 9
28 families and is dominated by *Carcharhinus* and *Carcharodon*. The occurrence of †*Hemipristis*
29 *serra* is of particular importance because it is the first Pleistocene record in the area. We
30 highlight high numbers of large *Carcharodon carcharias* in our sample exceeding 4 m, along
31 with the diverse fossil elasmobranchs, suggesting that a once rich and thriving marine ecosystem
32 in an inshore to offshore shallow-water environment during the early Pleistocene in Taiwan.

33

34 **Introduction**

35 The Indo-West Pacific is regarded as one of the crucial marine biodiversity hotspots in the world
36 (Myers et al., 2000; Bellwood & Meyer, 2009). Most of the species are concentrated in the coral
37 triangle area that has its northern limit extending to southern Taiwan. A remarkable 181
38 chondrichthyan species have been recorded in the modern fish fauna of Taiwan (Ebert et al.,
39 2013), approximating over 15% of the total number of global chondrichthyan species

40 (Weigmann, 2016). Such species diversity is regarded as one of the highest biodiversity hotspots
41 for elasmobranchs when considering the size of Taiwan (Ebert et al., 2013). However, how this
42 remarkable chondrichthyan fauna was formed and evolved in the past are not well understood,
43 primarily because relevant fossil records are traditionally overlooked or unstudied, despite being
44 well-represented in the marine deposits of Taiwan. Thus, comparisons for associated fossil fauna
45 and past biogeographic distributions are limited, particularly in the tropical-subtropical Pacific.
46 Lin et al. (2021) highlighted the need for paleontological data for understanding the historical
47 context of fish fauna and further recommended research potentials in the region.

48

49 In the Western Foothills of Taiwan, numerous Neogene to Quaternary strata are known to be rich
50 in marine fossils (e.g., Ribas-Deulofeu, Wang & Lin, 2021; Lin & Chien, 2022; Lin et al., 2022).
51 In particular, the early Pleistocene Liuchungchi Formation in the Niubu area, Chiayi County,
52 southwestern Taiwan is of particular research interest due to its abundance and diversity of
53 marine fauna. The fauna includes mollusks (Hu, 1989; Xue, 2004), crabs (Hu, 1989; Hu & Tao,
54 1996, 2004; Xue, 2004), sea urchins (Hu, 1989; Xue, 2004), whale barnacles (Buckeridge, Chan
55 & Lee, 2018), teleost (Tao, 1993) and otoliths (Lin et al., 2018), and elasmobranch teeth (Xue,
56 2004). Fossils from this area have been collected by the late W.-J. Xue during the 1980s-2000s,
57 and currently this large and diverse collection (over 3,000 specimens) is mainly deposited in the
58 Chiayi Municipal Museum, Chiayi City, Taiwan (CMM). There is a considerable number of
59 elasmobranch teeth from Xue's collection that were partly reported by Xue (2004) in a form of
60 photographic atlas without descriptions. Another collection donated by Prof. Hsi-Jen Tao
61 (National Taiwan University) to the Biodiversity Research Museum, Academia Sinica, Taipei,
62 Taiwan (BRMAS) is available. An additional small collection is also deposited in the National
63 Taiwan Museum (NTM). The purpose of this present study is to properly document the
64 occurrences of these elasmobranch fossils from the Liuchungchi Formation at the Niubu locality
65 based on these two collections and few newly collected specimens. The diverse association of
66 teeth provides opportunities for obtaining a more complete view of the Pleistocene elasmobranch
67 fauna in the rarely explored subtropical West Pacific.

68

69 **Geological setting**

70 Since the late Miocene, the island of Taiwan was gradually uplifted by the Penglai orogeny—the
71 collision between the Chinese continental margin and the Luzon Arc—and, subsequently, a
72 series of subsiding foreland basins were formed in western Taiwan (Ho, 1976; Suppe, 1984;
73 Lundberg et al., 1997; Lin & Watts, 2002; Nagel et al., 2013; Chen, 2016). These foreland basins
74 gradually developed from north to south accumulating clastic sediments (Ho, 1967; Covey,
75 1984; Teng, 1990), and in the south, the basins have high deposition rates (700–900 m/Ma) due
76 to a deeper depositional environment (Chen, Huang & Yang, 2011). Thus, the depositional
77 sequences reflect sea-level changes during the Quaternary that followed the 100 ky orbit
78 eccentricity cycles (Chen, Huang & Yang, 2011; Chen, 2016). Meanwhile, thick pre-orogenic
79 and synorogenic sediments infilling the foreland basin were squeezed and uplifted, which formed

80 the 7–9 km Miocene to Pleistocene strata in the Western Foothills (Yu & Chou, 2001; Nagel et
81 al., 2013).

82

83 The Liuchungchi Formation in the Niubu area, Chiayi County is exposed along the Bazhang
84 River (Fig. 1B). Four successive formations from east to west, lower to upper can also be
85 observed along this river: the Liuchungchi, Kanhsialiao, Erhchungchi, and Liushuang formations
86 (Stach, 1957; Chou, 1975; Chen, Huang & Yang, 2011; Chen, 2016; Fig. 1B, C). The age of the
87 Liuchungchi Formation is 1.90–1.35 Ma (Chen, 2016), with a deposition rate of about 700 m/Ma
88 in the lower section and 1,100 m/Ma upsection, the maximum thickness of the formation is 760
89 m (Chen, Huang & Yang, 2011). The Liuchungchi Formation is composed of dozens of
90 depositional sequences, each representing a 41 ky climate cycle (Chen, Huang & Yang, 2011;
91 Chen, 2016). The depositional environment can be divided into two distinct sections, with the
92 lower sequence composed of thick sandstone with cross bedding, parallel bedding, and strong
93 bioturbation reflecting shoreface to the offshore transition zone, and the upper sequence
94 composed of interbeds of sandstone and shale and storm deposits in the form of sandstone,
95 indicating the inner offshore (Chen, Huang & Yang, 2011; Chen, 2016).

96

97 Materials & Methods

98 The fossil site is located in the Niubu area, Chiayi County, southwestern Taiwan, about 15 km
99 east of Chiayi City (Fig. 1A). The layers containing fossils are exposed along the Bazhang River,
100 just downstream of a dam near a high-voltage tower, where they are readily accessible during the
101 winter and dry seasons when the water level is low (Supplemental Fig. S1). Fossil mollusks are
102 very abundant in several of the condensed layers, as well as fragments of crabs, sea urchins, and
103 teleost fish bones (Fig. 2A). Fossil shark teeth are rare based on both surface collecting and bulk
104 sampling conducted during our several field trips in 2018–2022. Bulk sediment samples of over
105 830 kg (Sites 1–3 in Fig. 2B) were sieved (500-μm mesh) from the loosely cemented siltstone
106 without any sedimentary structure, yielding a large number of otoliths (Lin et al., unpublished
107 data), but only one shark tooth and two ray teeth. We note the discrepancy in the numbers of
108 elasmobranch specimens between museum collections and our field surveys is present, and it is
109 explained by the fact that the larger sample sizes in museum collections primarily reflect
110 collecting based on fortuitous occurrences of shark teeth over the past 3–4 decades, compared to
111 collecting based on our limited number of field surveys. Moreover, the initial purpose of the bulk
112 sampling was for collecting teleost otoliths instead of elasmobranch teeth, and these selected
113 sites contained more otoliths than teeth.

114

115 The upstream of Bazhang River contains strata older than the Liuchungchi Formation; these
116 include the Neogene Tangenshan Sandstone and Yenshukeng Shale, which are exposed
117 approximately 1 km east to the weir (Figs. 1, 2), with an elevation of more than 300 m compared
118 to the level of our sampling sites. Both stratigraphic units are composed of consolidated
119 sandstones with some marine fossils such as mollusks, but these are different from the fine,

120 unconsolidated siltstones of the Liuchungchi Formation. After storms and rainy seasons,
121 numerous blocks of sandstones from these older strata can be found along the riverbed of the
122 Bazhang River (Supplemental Fig. S1), but these lithologically distinct rocks are confined to
123 areas below our sampling sites. We thus consider that the mixing of older Neogene fossils with
124 our Pleistocene specimens is improbable, and that our assemblage represents fossils derived
125 entirely from the Liuchungchi Formation.

126

127 The BRMAS, CMM, and NTM collections analyzed here were collected from the surface
128 exposure of the Niubu locality without bulk-sampling of sediments; however, the exact
129 stratigraphic horizons and detailed lithologic character within the Liuchungchi Formation for
130 each specimen are not known. Stacked images of teeth were taken and measurements of crown
131 height (CH), mesial crown edge length (MCL), and basal crown width, (BCW) were noted
132 wherever necessary. Specimens from the BRMAS are registered under ASIZF, CMM under
133 CMM F, and those in the NTM are under NTM I. Because the Pleistocene is relatively close to
134 modern times, the morphology of elasmobranch teeth has not changed much from that time to
135 the present. Therefore, identifications of these fossil teeth were conducted by comparing them
136 with teeth of extant taxa.

137

138 The diversity of our elasmobranch assemblage was compared with other Pleistocene
139 assemblages to highlight its significance within the associated spatio-temporal context.
140 Taxonomic composition and abundance data from the early Pleistocene temperate assemblages
141 of Japan (Karasawa, 1989; Kawase & Nishimatsu, 2016; Tanaka & Taru, 2022) and tropical
142 records from Java (Koumans, 1949; Yudha et al., 2018) and Sulawesi (Hooijer, 1954) were
143 extracted. We calculated diversity indices, including species richness, Shannon's entropy,
144 Simpson's diversity index, and Fisher's alpha for a general comparison.

145

146 Systematic Paleontology

147 A summary of taxa and their numeric abundance are listed in Table 1. The elasmobranch
148 assemblage contains 697 teeth, consisting of 9 families and 20 taxa. The classification scheme
149 follows that of Nelson, Grande & Wilson (2016), except for the family Galeocerdonidae, which
150 we follow Fricke, Eschmeyer & Van der Laan (2022). General morphological terminology
151 follows that of Compagno (1984, 2002), Purdy et al. (2001), Shimada (2002), Purdy (2006),
152 Cappetta (2012), and Ebert et al. (2013). The synonymy list is limited to relevant records from
153 Taiwan (Huang, 1965; Uyeno, 1978; Hu & Tao, 1993; Xue, 2004; Tao & Hu, 2008).

154

155 Class Chondrichthyes Huxley, 1880
156 Order Lamniformes Berg, 1958
157 Family Carchariidae Müller & Henle, 1838
158 Genus *Carcharias* Blainville, 1816
159 *Carcharias taurus* Rafinesque, 1810

160 (Fig. 3)

161

162 1978 *Odontaspis* sp.; Uyeno, pl. 1, fig. 5.

163

164 **Referred specimens:** n = 2: ASIZF0100320, CMM F0204.

165 **Description:** CH = 12.92–16.83 mm; MCL = 12.18–15.54 mm; BCW = 7.07–7.84 mm. The
166 teeth are characterized by a slender, dagger-like main cusp and a single pair of small lateral
167 cusplets. The crown exhibits no serrations. The lingual protuberance of the root is prominent.

168 **Remarks:** The teeth of *Carcharias taurus* are similar to those of *Odontaspis noronhai* and *O.*
169 *ferox* by having a slender main cusp and lateral cusplet. However, the lateral cusplets of
170 *Odontaspis* are more pronounced than those of *C. taurus*, including the fact that teeth of *O. ferox*
171 typically exhibit multiple pairs of lateral cusplets.

172

173

174 **Genus** *Carcharodon* Smith, 1838

175 *Carcharodon carcharias* (Linnaeus, 1758)

176 (Fig. 4)

177

178 1978 *Carcharhinus* sp.; Uyeno, pl. 1, fig. 4, pl. 2, fig. 7.

179 1978 *Carcharodon carcharias*; Uyeno, pl. 3, figs. 12, 13.

180 2004 *Elasmobranchii* indet.; Xue, pl. 1, figs. 1–6, pl. 2, figs. 1–7, pl. 3, figs. 1, 2–7, pl. 7 fig. 2.

181

182 **Referred specimens:** n = 55: ASIZF0100322–0100346, 0100435, 0100465, 0100530. CMM
183 F0001–F0005, F0007–F0010, F0012–F0022, F0210, F0212, F2824, F2825, F2830, NTM
184 I01122, I01123.

185 **Description:** CH = 6.76–41.03 mm; MCL = 9.61–45.68 mm; BCW = 8.74–37.09 mm. The
186 upper teeth (Fig. 4A–N) are broad and triangular. The cutting edge of both mesial and distal
187 sides is almost straight with coarse serrations. The labial face of the crown is flat and the lingual
188 face is convex, where the crown is erect and symmetric to slightly distally inclined depending on
189 tooth positions. The root is slightly arched, and the nutritive foramina and transverse groove are
190 not prominent or absent. The lower teeth (Fig. 4O–X) have a more robust but narrower serrated
191 crown and bilobate roots with a rounded lingual face compared to the upper teeth.

192 **Remarks:** The genus *Carcharodon* is represented by three species: †*C. hastalis*, †*C. hubbelli*,
193 and *C. carcharias*. Whereas *C. hastalis*, which was traditionally placed in the genus *Isurus* or
194 †*Cosmopolitodus*, lived through the Miocene and early Pliocene, †*C. hubbelli* in the late
195 Miocene and *C. carcharias* in the early Pliocene–Recent form a single lineage of chronospecies
196 by developing serrations on their teeth (Ehret et al., 2012). The specimens described in this
197 present paper exhibit well-developed serration consistent with teeth of *C. carcharias* (e.g.,
198 Hubbell, 1996), and not like the teeth of *C. hubbelli* with weak serrations (Ehret et al., 2012).

199 They include the largest dental remains among all the shark tooth specimens described in this
200 paper.

201

202 Genus *Isurus* Rafinesque, 1810

203 *Isurus oxyrinchus* Rafinesque, 1810

204 (Fig. 5)

205

206 ?1965 *Isurus hastalis*; Huang, pl. 22, figs. 12–14.

207 1993 *Isurus hastalis*; Hu & Tao, pl. 24, figs. 6, 8.

208 2004 *Elasmobranchii* indet.; Xue, pl. 5, fig. 3, pl. 8, fig. 4.

209 2008 *Isurus* sp.; Tao & Hu, pl. 2, figs. 1–2.

210

211 **Referred specimens:** n = 6: ASIZF0100317–0100319, 0100321, CMM F0242, NTM I01131_1.

212 **Description:** CH = 9.86–27.81 mm; MCL = 12.21–26.89 mm; BCW = 9.31–9.96 mm. The
213 **mesial** teeth have a slender, dagger-like, unserrated crown that is erect or lingually curved with
214 an apical labial flexure (Fig. 5A–H). The root, if preserved, has two rather narrow lobes with a
215 moderately tight basal concavity. The **distal** teeth have a flatter and broader, distally curved,
216 unserrated crown with a short but mesiodistally wide root (Fig. 5I, J).

217 **Remarks:** Two extant species of *Isurus* are known: *I. oxyrinchus* and *I. paucus*. *Isurus*
218 *oxyrinchus* has a more elongated and more labially curved crown than *I. paucus* (Whitenack &
219 Gottfried, 2010). The teeth of *I. oxyrinchus* are also similar to those of *Carcharias taurus*, but the
220 teeth of *C. taurus* have a pair of lateral cusplets that is absent in the teeth of *I. oxyrinchus*
221 (Wilmers, Waldron & Bargmann, 2021). Huang (1965) reported a tooth of †*I. hastalis* (=
222 *Carcharodon hastalis*; see above) from the Pleistocene Cholan Formation in Hsinchu, northern
223 Taiwan; however, **its** species identification is questionable and the whereabouts of the specimens
224 is unknown for verification.

225

226 Order Carcharhiniformes Compagno, 1973

227 Family Hemigaleidae Hasse, 1878

228 Genus *Hemipristis* Agassiz, 1835

229 †*Hemipristis serra* Agassiz, 1843

230 (Fig. 6)

231

232 1978 *Hemipristis serra*; Uyeno, pl. 1, fig. 2.

233 2004 *Hemipristis* sp.; Xue, pl. 5, figs. 1, 2, 5, 6, 7.

234 2004 *Elasmobranchii* indet.; Xue, pl. 5, fig. 5, pl. 7, figs. 3, 5, pl. 9, figs. 6, 7.

235 2008 *Hemipristis serra*; Tao & Hu, pl. 6, fig. 1.

236

237 **Referred specimens:** n = 7: ASIZF0100460–0100462, CMM F0232, F2826, F2827, NTM

238 I01131_2.

239 **Description:** CH = 5.21–30.81 mm; MCL = 8.73–41.38 mm; BCW = 6.50–36.59 mm. All
240 collected specimens of this taxon represent upper teeth that are characterized by a distally
241 inclined, broad triangular crown, and mesiodistally separated bilobate root. Coarse serrations are
242 present along the distal cutting edge, whereas serrations along the meosal cutting edge are finer.
243 The root has a prominent lingual protuberance with a deep nutritive groove, and has a notch-like
244 shallow basal concavity. The crown overhangs the root, and their boundary, especially on the
245 lingual face, is strongly arched.

246 **Remarks:** As presumed sister species, the teeth of extinct *†Hemipristis serra* and extant *H.*
247 *elongata* are similar. However, compared to *†H. serra*, teeth of *H. elongata* possess a more
248 gracile crown and a longer apex without serration, and a narrower root (Smith, 1957; Purdy et
249 al., 2001). The Pleistocene records of *†H. serra* are rare globally compared to its Neogene
250 records (Hooijer, 1954, 1958; Yabumoto & Uyeno, 1994; Carrillo-Briceño et al., 2015; Ebersole,
251 Ebersole & Cicimurri, 2017; Boessenecker, Boessenecker & Geisler, 2018).

252

253 Family Carcharhinidae Jordan & Evermann, 1896

254 Genus *Carcharhinus* Blainville, 1816

255

256 **Remarks:** The identification based on teeth below the genus level is difficult for *Carcharhinus*
257 (Compagno, 1984, 1988; Purdy et al., 2001; Naylor & Marcus, 1994; Marsili, 2006; Voigt &
258 Weber, 2011; Ebert, Dando & Fowler, 2021). Most of the upper teeth are triangular with their
259 crown inclining distally. In different species, the crown varies from narrow to broad, and has
260 smooth to coarsely serrated cutting edges, different notch angles on distal cutting edges, and the
261 straight to convex mesial cutting edge. At least nine species of *Carcharhinus* are recorded in the
262 collections: *C. altimus*, *C. amboinensis*, *C. leucas*, *C. limbatus*, *C. longimanus*, *C. obscurus*, *C.*
263 *plumbeus*, *C. sorrah*, and *C. tjtjot*. See remarks below for comparisons among other similar-
264 looking species.

265

266 *Carcharhinus altimus* (Springer, 1950)

267 (Fig. 7)

268

269 **Referred specimens:** n = 17: ASIZF0100357, 0100359, 0100362, 0100363, 0100365, CMM
270 F0080, F0101, F0113, F0134, F0214, F0224, F0293, F0304, F0322, F0363, TNM I01125,
271 I01129_1.

272 **Description:** CH = 4.55–9.82 mm; MCL = 7.91–12.72 mm; BCW = 7.10–10.92 mm. The
273 specimens examined in this study consist only of upper teeth. The crown of the upper teeth is
274 finely serrated and varies in shape from a tall triangle to distally oblique. There is a notch on the
275 distal cutting edge, whereas a slight constriction occurs on the lower part of the mesial cutting
276 edge. The root is arched and has a nutritive groove. The roots of some specimens are not well-
277 preserved (Fig. 7A, B, E, F, I–L), but where well-preserved (Fig. 7C, D, G, H), it is arched and
278 exhibits a nutritive groove on the lingual face.

279 **Remarks:** Teeth of *Carcharhinus altimus* and *C. plumbeus* are similar. However, those of *C.*
280 *altimus* exhibit a distally bent apex unlike those of *C. plumbeus* that show an apically directed
281 apex (Figs. 7 vs. 13).

282

283 *Carcharhinus amboinensis* (Müller & Henle, 1839)
284 (Fig. 8)

285

286 **Referred specimens:** n = 5: ASIZF0100366, 0100368, 0100369, CMM F0209, F0229.

287 **Description:** CH = 6.88–8.95 mm; MCL = 9.28–14.74 mm; BCW = 9.16–16.86 mm. The
288 triangular crown is broad and exhibits coarse serrations although the serrations become smaller
289 towards the apex. A prominent tooth neck is present between the crown and root on the lingual
290 face. There is a notch on the distal cutting edge, whereas the mesial cutting edge is nearly
291 straight. The bilobed root is gently arched and has a nutritive groove on the lingual face.

292 **Remarks:** Teeth of *Carcharhinus amboinensis*, *C. leucas*, and *C. longimanus* are very similar
293 (Marsili, 2006; Voigt & Weber, 2011). However, the angle of the notch on the distal cutting edge
294 of *C. longimanus* is larger than *C. leucas* and *C. amboinensis*. Compared to the teeth of *C.*
295 *leucas*, the upper teeth of *C. amboinensis* are somewhat broader, the crowns are generally lower
296 and more distally curved, and their distal heel is more pronounced and is closer to the base of the
297 crown (Kocsis et al., 2019).

298

299 *Carcharhinus leucas* (Valenciennes, 1839)
300 (Fig. 9)

301

302 ?1965 *Carcharhinus gangeticus*; Huang, pl. 22, figs. 19, 20.

303 2004 *Elasmobranchii* indet.; Xue, pl. 3, fig. 2, pl. 4, fig. 3, pl. 7, fig. 7, pl. 9, fig. 4.

304

305 **Referred specimens:** n = 71: ASIZF0100390, 0100393–0100398, 0100400–0100404, 0100411,
306 0100419, 0100424, 0100425, 0100481, CMM F0154, F0155, F0157, F0159, F0162, F0163,
307 F0165–F0168, F0170–F0175, F0180, F0183, F0186–F0188, F0190, F0192, F0198–F0201,
308 F0205, F0206, F0221, F0222, F0227, F0231, F0240, F0244, F0246, F0249, F0288, F0290,
309 F0297, F0299, F0301, F0317, F0319, F0321, F0328, F0332, F0334, F0341, F0342, F0348,
310 F0354, F0362, NTM I01130_2.

311 **Description:** CH = 4.87–18.68 mm; MCL = 7.97–21.69 mm; BCW = 8.73–30.56 mm. The teeth
312 of *Carcharhinus leucas* are generally robust. The crown of the upper teeth (Fig. 9A–P) is broad
313 and triangular with a slight distal inclination. The middle of the distal cutting edge is concave,
314 forming a weak notch, whereas the mesial cutting edge is straight to slightly convex. Both
315 cutting edges are coarsely serrated, but the sizes of serrations are smaller at the base and apex of
316 the crown than those in the middle. The boundary between the crown base and root on the
317 lingual face displays a V-shape tooth neck. The bilobate root is arched and displays a weak

318 nutritive groove on the lingual face (Fig. 9A–H, K, L). The lower teeth (Fig. 9Q, R), that have
319 fine serrations, are labiolingually thicker and mesiodistally narrower than the upper teeth.
320 **Remarks:** Marsili (2006) described the crown of *Carcharhinus longimanus* as larger, more
321 elongate and possessing a straighter root margin compared to that of *C. leucas*. In addition, based
322 on the images of *Carcharhinus* by Garrick (1982) and Voigt & Weber (2011), we find some
323 other slight differences in tooth morphology between the two species. For example, the angle on
324 the distal cutting edge of the upper teeth in *C. longimanus* is larger than that in *C. leucas*, making
325 the crown of *C. leucas* incline more distally than that in *C. longimanus*. In addition, the tooth
326 shape of *C. leucas* is close to a wide-bottom triangle, whereas that of *C. longimanus* forms a
327 taller triangle. Furthermore, the lower teeth of *C. leucas* tend to exhibit a stronger demarcation
328 between the main cusp and mesial and distal heels than those of *C. longimanus* with a smoother
329 cusp-heel transition.

330

331 *Carcharhinus limbatus* (Valenciennes, 1839)

332 (Fig. 10)

333

334 1978 *Carcharhinus* sp.; Uyeno, pl. 3, fig. 14.

335 2004 *Elasmobranchii* indet.; Xue, pl. 8, fig. 5.

336

337 **Referred specimens:** n = 40: ASIZF0100467–0100480, 0100482, 0100483, CMM F0056,
338 F0111, F0216, F0217, F0234, F0236–F0238, F0286, F0289, F0291, F0295, F0306, F0307,
339 F0310, F0368–F0373, NTM I01127, I01133_2, I01134_2.

340 **Description:** CH = 7.70–9.31 mm; MCL = 10.02–13.26 mm; BCW = 10.26–14.70 mm. Our
341 specimens consist only of upper teeth. The teeth of *C. limbatus* are serrated and are characterized
342 by a narrow cusp that is erect to slightly oblique distally with a mesiodistally wide crown base.
343 The serrations near the crown base are coarser than those towards the apex. The root is
344 apicobasally shallow. Its base is straight to slightly arched with a prominent deep nutritive
345 groove that forms a notch along the root base.

346 **Remarks:** Although similar, teeth of *Carcharhinus limbatus* can be distinguished from those of
347 *C. amblyrhynchos*, *C. brachyurus* and *C. brevipinna*. Unlike the teeth of *C. limbatus*, the
348 serrations on the cutting edges tend not to continue to the crown base in *C. amblyrhynchos*, and
349 are absent or weak in *C. brevipinna*, and in *C. brachyurus*, the apex is more pointed and more
350 distally directed than in *C. limbatus* (Garrick, 1982; Voigt & Weber, 2011). In addition, the
351 crowns of *C. limbatus* have a narrow, erect cusp with a sharp transition to their broad crown base
352 that is distinct from all other congeneric specimens in our material. The teeth of *C. limbatus* and
353 *C. amblyrhynchos* are, however, very difficult to distinguish. Kocsis et al. (2019) noted a
354 narrower crown with finer serrations in *C. limbatus*, but this character is not clear in our
355 specimens. Currently, no records of *C. amblyrhynchos* have been reported in Taiwan (Ebert et
356 al., 2013; Shao, 2022); therefore, we tentatively assign these specimens to *C. limbatus*.

357

358 *Carcharhinus longimanus* (Poey, 1861)

359 (Fig. 11)

360

361 1965 *Carcharhinus gangeticus*; Huang, pl. 22, figs. 21, 22.

362 2004 *Elasmobranchii* indet.; Xue, pl. 4, fig. 4, pl. 7, fig. 6, pl. 9, fig. 1.

363

364 **Referred specimens:** n = 36: ASIZF0100370, 0100371, 0100373–0100382, 0100391, 0100392, 0100421, 0100422, 0100428, 0100466, CMM F0006, F0011, F0087, F0151, F0153, F0156, F0158, F0182, F0189, F0194, F0195, F0197, F0223, F0248, F0287, F0294, NTM I01128, NTM I01130.

368 **Description:** CH = 10.23–15.93 mm; MCL = 13.51–22.08 mm; BCW = 13.20–21.69 mm. The 369 crowns of the upper teeth (Fig. 11A–P) are broad, triangular, and coarsely serrated. The distal 370 cutting edge is weakly concave, whereas the mesial cutting edge is nearly straight. The crown 371 base on the lingual side is deeply concave and is accompanied basally by a narrow tooth neck 372 and a deep bilobate root with a shallow nutritive groove. The lower teeth (Fig. 11Q–T) are 373 thicker and narrower than the upper teeth, they also have fine serrations on the cutting edges. The 374 boundary between the crown base and root on the lingual side is also deeply concave with a V- 375 shaped tooth neck.

376 **Remarks:** See remarks under *Carcharhinus leucas*.

377

378 *Carcharhinus obscurus* (Lesueur, 1818)

379 (Fig. 12)

380

381 2004 *Elasmobranchii* indet.; Xue, pl. 4, fig. 7.

382

383 **Referred specimens:** n = 25: ASIZF0100372, 0100383–0100389, 0100399, CMM F0123, 384 F0143, F0148, F0160, F0164, F0176–F0179, F0181, F0184, F0196, F0208, F0338, F0353, NTM 385 I1132_3.

386 **Description:** CH = 5.04–15.14 mm; MCL = 7.57–21.61 mm; BCW = 9.56–20.96 mm. The 387 specimens in this study consist only of upper teeth. They are broad and triangular with coarse 388 serrations, although the serrations tend to become finer apically. The mesial cutting edge is 389 overall slightly convex with a marked distally directed apex. The distal cutting edge has a 390 relatively deep notch, but the degree of the angle varies based on tooth positions █ within the 391 dentition. The crown base on the lingual side is moderately concave and is accompanied by a 392 prominent tooth neck and a relatively robust bilobed root that has a shallow nutritive groove.

393 **Remarks:** The crown of *Carcharhinus obscurus* is mesiodistally broad and typically exhibits 394 coarse serrations along the middle section of both cutting edges, a feature for separating all other 395 congeneric specimens in the present study.

396

397 *Carcharhinus plumbeus* (Nardo, 1827)

398 (Fig. 13)

399

400 **Referred specimens:** n = 51, ASIZF0100405–0100410, 0100412, 0100429, CMM F0074–
401 F0077, F0079, F0086, F0088, F0091, F0096, F0100, F0106, F0115, F0124, F0144, F0146,
402 F0169, F0225, F0228, F0292, F0302, F0316, F0318, F0320, F0325–F0327, F0330, F0331,
403 F0333, F0335, F0337, F0346, F0347, F0349, F0350, F0352, F0356, F0360, F0361, F0364,
404 F0365, F0367, NTM I01124.

405 **Description:** CH = 6.28–12.17 mm; MCL = 7.81–17.06 mm; BCW = 7.48–13.39 mm. The teeth
406 that are referred to this species are all upper teeth. They are triangular with a slight distal
407 inclination and with fine serrations. The mesial cutting edge is nearly straight, whereas the distal
408 cutting edge tends to form a shallow notch close to the crown base. The root is bilobate and
409 arched, and a shallow nutritive groove is present on the lingual face.

410 **Remarks:** The crown of *Carcharhinus plumbeus* is narrower and elongate than that of *C. leucas*, *C. longimanus*, *C. obscurus*, and *C. amboinensis*, but it is wider than that of *C. altimus*.

412

413 *Carcharhinus sorrah* (Valenciennes, 1839)

414 (Fig. 14)

415

416 **Referred specimens:** n = 11: ASIZF0100418, CMM F0117, F0119, F0122, F0126, F0129,
417 F0135, F0140, F0303, F0343, F0344.

418 **Description:** CH = 4.39–5.80 mm; MCL = 5.55–9.82 mm; BCW = 4.03–9.85 mm. All teeth
419 identified to this species are represented by upper teeth. Their crown consists of a finely serrated
420 triangular cusp that strongly inclines distally along with a coarsely serrated, relatively broad
421 distal heel. The apex is narrow and may be slightly recurved apically (Fig. 14E–H). The
422 serrations on the distal heel become smaller distally, where finer secondary serrations are
423 observed on one or two of the mesial-most serrations. Well-preserved specimens exhibit a strong
424 nutritive groove on the lingual face that forms a notch along the root base.

425 **Remarks:** According to Voigt & Weber (2011), the crown of the upper teeth in *Carcharhinus*
426 *sorrah* is high, and its distal cutting edge is deeply notched. These features are seen in our
427 specimens, but their descriptions for the serrations are slightly different. The serrations on the
428 central part of the mesial cutting edges are coarser in Voigt & Weber (2011), whereas in our
429 specimens, the coarsest serrations are on the basal part of the mesial cutting edges. Furthermore,
430 the main cusp and coarse serrations in our specimens are farther apart than those figured by
431 Voigt & Weber (2011). The teeth of *C. tjutjot* and *C. sorrah* are both characterized by a coarsely
432 serrated distal heel, but the teeth of *C. tjutjot* differ from those of *C. sorrah* by having fewer but
433 larger serrations forming a distal heel (Figs. 14 vs. 15).

434

435 *Carcharhinus tjutjot* (Bleeker, 1852)

436 (Fig. 15)

437

438 **Referred specimens:** n = 19: ASIZF0100413–0100417, CMM F0116, F0136–F0138, F0142,
439 F0296, F0298, F0323, F0324, F0339, F0345, F0357, F0376, F0377.

440 **Description:** CH = 4.25–5.82 mm; MCL = 6.03–9.01 mm; BCW = 5.61–7.94 mm. The
441 specimens of this species described here are all represented by upper teeth. They have a robust,
442 distally inclined, triangular cusp, a small distal heel consisting of coarse serrations that rapidly
443 diminish in size distally. The strongly inclined mesial cutting edge is relatively straight, where
444 the apex may slightly recurve apically and its serrations become slightly coarser towards the
445 base. Finer secondary serrations are observed on the first and possibly second mesial-most
446 serrations on the distal heel. The root is weakly bilobate as the root base is nearly straight. Well-
447 preserved specimens show a shallow nutritive groove on the lingual face of the root.

448 **Remarks:** The teeth of *Carcharhinus sealei*, *C. dussumieri*, *C. coatesi*, and *C. tjutjot* are very
449 similar (White, 2012). The differences among them are the serrations on the cutting edges. The
450 serrations of *C. sealei* are present only on the basal half of the mesial cutting edge, where the
451 distal cutting edge, including the distal heel, is smooth (White, 2012). Both cutting edges of teeth
452 in *C. coatesi* have fine to coarse serrations, but their distal heel is smooth. In *C. dussumieri*, both
453 cutting edges of teeth, including the distal heel, have evenly-sized coarse serrations. The teeth of
454 *C. tjutjot* also have evenly-sized serrated cutting edges, including the distal heel. *Carcharhinus*
455 *dussumieri* and *C. tjutjot* have long been misidentified due to their similar appearance, but *C.*
456 *dussumieri* is now considered a West Indian species distributed from the Persian Gulf to India,
457 whereas *C. tjutjot* is distributed from Indonesia to Taiwan (White, 2012).

458

459 Genus *Rhizoprionodon* Whitley, 1929

460 *Rhizoprionodon acutus* (Rüppell, 1837)

461 (Fig. 16)

462

463 Referred specimens: n = 8: ASIZF0100463, 0100464, CMM F0110, F0120, F0121, F0130,
464 F0131, F0218.

465 **Description:** CH = 3.97–5.35 mm; MCL = 6.22–10.82 mm; BCW = 7.68–10.69 mm. The upper
466 teeth of this species have a crown that is strongly inclined distally and is accompanied by a low
467 distal heel (Fig. 16A–H). Both cutting edges, including the distal heel, are smooth or exhibit fine
468 irregular serrations. The mesial cutting edge is overall straight, whereas the junction between the
469 cusp and distal heel is deeply notched. A deep nutritive groove is present on the lingual side of
470 the root that continues to the root base. The root is low with little to no basal concavity.

471 ASIZF0100464 (Fig. 16I, J) is a lower tooth, where its crown that is unserrated is more gracile
472 than the upper teeth with a concave mesial cutting edge. The root morphology is similar to that
473 of lower teeth.

474 **Remarks:** The teeth of *Rhizoprionodon acutus* are serrated in adults (Compagno, 1984). In our
475 specimens, the serrations are absent, indicating immature individuals. Distinguishing between
476 the teeth of *R. acutus* and *R. oligolinx* is difficult, where both have very fine irregular serrations.

477 However, due to the questionable distribution of *R. oligolinxi* in Taiwan (Ebert et al., 2013;
478 Froese & Pauly, 2022), we tentatively assign these specimens to *R. acutus*.

479

480 Family Galeocerdonidae *sensu* Ebersole, Cicimurri & Stringer, 2019

481 Genus *Galeocerdo* Müller & Henle, 1837

482 *Galeocerdo cuvier* (Péron & Lesueur, 1822)

483 (Fig. 17A–H)

484

485 ?1965 *Galeocerdo aduncus*; Huang, pl. 22, figs. 10, 11.

486 ?1978 *Galeocerdo aduncus*; Uyeno, pl. 1, fig. 3.

487 2004 *Elasmobranchii* indet.; Xue, pl. 6, figs. 1–7, pl. 8, fig. 6.

488

489 **Referred specimens:** n = 7: ASIZF0100459, CMM F0213, F0215, F0245, F2823, F2829, NTM
490 I01121.

491 **Description:** CH = 12.27–17.72 mm; MCL = 17.37–26.88 mm; BCW = 18.10–28.05 mm. The
492 teeth of *G. cuvier* are characterized by a coarsely serrated crown with a cusp that strongly curves
493 distally and a prominent distal heel demarcated by a deep notch at approximately 90 degrees
494 angle along the distal cutting edge. Fine secondary serrations are present on the coarser primary
495 serrations (Fig. 17E, H). The serrations on the distal heel in ASIZF0100459 (Fig. 17F,G) are
496 weak, the width to crown height ratio suggests this tooth represents a posterior position. CMM
497 F0245 and CMM F0215 are anterior teeth with well-marked serration (Fig. 17A–D).

498 **Remarks:** Five extinct species and one extant species of *Galeocerdo* are considered valid: the
499 Eocene †*G. clarkensis* and †*G. eaglesomei*, Oligocene–late Miocene †*G. aduncus*, Miocene †*G.*
500 *mayumbensis*, Pliocene †*G. capellini*, and the Pleistocene–Recent *G. cuvier* (Purdy et al., 2001;
501 Türtscher et al., 2021). The specimens described here are identified as *G. cuvier*, particularly
502 because of the presence of secondary serrations (Cigala-Fulgosi & Mori, 1979; Türtscher et al.,
503 2021). Huang (1965) reported a questionable occurrence of †*G. aduncus* from the Pleistocene
504 Cholan Formation in Hsinchu, northern Taiwan, however we consider the specimen lost. Uyeno
505 (1978) reported another occurrence of †*G. aduncus* from the poorly constrained Plio-Pleistocene
506 strata along the Tsailiao River in Tainan, southwestern Taiwan (as Miocene to Pleistocene in
507 Uyeno, 1978). Although Uyeno's collection was deposited in the NTM, we were not able to
508 locate the specimen of †*G. aduncus* in the collection. Nevertheless, although the whereabouts of
509 the specimen is uncertain, it is interpreted here to have also belonged to *G. cuvier*.

510

511 Family Sphyrnidae Bonaparte, 1840

512 Genus *Sphyrna* Rafinesque, 1810

513 *Sphyrna lewini* (Griffith & Smith, 1834)

514 (Fig. 17I–L)

515

516 ?1978 *Sphyrna* sp.; Uyeno, pl. 2, fig. 8

517

518 **Referred specimens:** n = 2: CMM F0235, F0312.

519 **Description:** CH = 4.64–6.85 mm; MCL = 7.51–11.17 mm; BCW = 7.19–10.53 mm. The tooth
520 crown of *S. lewini* is characterized by a **slender** distally inclined cusp with a narrow, mesially
521 extended base separated by a slight concavity along the mesial cutting edge and a low distal heel
522 demarcated by a deep notch. Both cutting edges are smooth without serrations. The root is **low**,
523 and its base is straight. It has a deep nutritive groove on the lingual side and extends to the root
524 base.

525 **Remarks:** The teeth of *Sphyrna lewini* are most similar to *S. macrorhynchos* and *Loxodon*
526 *macrorhinus*, but a slight concavity is present on the base of the mesial cutting edge in *S. lewini*,
527 whereas the edge is almost straight in the latter two species (Ebert et al., 2013).

528

529 Order Myliobatiformes Compagno, 1973

530 Family Dasyatidae Jordan & Gilbert, 1879

531 Dasyatidae indet.

532 (Fig. 18)

533

534 **Referred specimens:** n = 2: ASIZF0100590, 0100591.

535 **Description:** The specimens are roughly hexagonal with a globular, thick crown and a well-
536 divided bilobed root that is smaller than the crown and extends ventrally. The **apex of the crown**
537 in both specimens is flat, but the specimen ASIZF0100590 (Fig. 18A–D) has blunt, rounded
538 corners compared to ASIZF0100591 (Fig. 18E–H).

539 **Remarks:** The teeth referred to this taxon may belong to the genus *Dasystis* or *Himantura*, but
540 because teeth of dasyatid taxa are highly variable in morphology, including sexual dimorphism
541 and differences in ornamentation pattern (Taniuchi & Shimizu, 1993; Kajiura & Tricas, 1996;
542 Herman, Hovestadt-Euler & Hovestadt, 1998, 1999, 2000), we refer our materials **simply** to
543 Dasyatidae indet. Uyeno (1978) reported teeth of *Dasyatis* sp. from the Miocene to Pleistocene
544 of Taiwan. However, whether our specimens are conspecific with Uyeno's (1978) specimens
545 cannot be ascertained.

546

547 Family Aetobatidae Agassiz, 1858

548 Genus *Aetobatus* Blainville, 1816

549 *Aetobatus* sp.

550 (Fig. 19)

551

552 **Referred specimens:** n = 58: ASIZF0100549–0100580, CMM F0380, F0382, F0388, F0395,

553 F0399–0409, F0412, F2848–F2850, F2852–F2854, NTM I01116, I01117, I01119, I01120.

554 **Description:** Teeth of *Aetobatus* are characterized by strongly extended roots on the lingual
555 (posterior) side and the arcuate crown in apical view with a flat occlusal surface. The crown
556 overhangs the root on the labial (anterior) side and the root is more prominent than the crown on

557 the lingual side. Both lingual and labial crown faces have fine vertical grooves as ornamentation.
558 The root is polyaulocorhizous, consisting of anteroposteriorly oriented, densely packed, vertical
559 lamellar plates.

560 **Remarks:** Five species of Myliobatidae (one *Aetobatus*, three *Aetomylaeus*, and one *Myliobatis*)
561 are known from Taiwan (Ebert et al., 2013). All of which have grinding-type dental plates but
562 each with different shapes and forms. The upper medial teeth of *Aetobatus ocellatus* are straight
563 and elongate but slightly distally deflected towards the lingual side; its lower teeth are strongly
564 arched towards the labial side. Considerable ontogenetic morphological change in dental **plate** is
565 known in *Aetomylaeus* (Hovestadt & Hovestadt-Euler, 2013). Both upper and lower dental plates
566 of adult *Aetomylaeus* are similar to the upper teeth of *Aetobatus*. Unlike adult individuals that
567 have a single row of medial teeth, juveniles of *Aetomylaeus* have one medial, two lateral, and
568 one posterior tooth **rows** (Hovestadt & Hovestadt-Euler, 2013). The hexagon shape of medial
569 teeth is very similar to those of juvenile *Myliobatis* (Hovestadt & Hovestadt-Euler, 2013). Teeth
570 of *Aetobatus* have weak ornaments on the labial and lingual crown, but in *Aetomylaeus*, beaded
571 ridges with reticulated and pitting patterns are observed (Ebersole, Cicimurri & Stringer, 2019).
572 Moreover, *Aetobatus* has teeth with a strong arched appearance than other myliobatid genera (see
573 also remarks under *Myliobatis* sp.).

574

575 Family Myliobatidae Bonaparte, 1835

576 Genus *Myliobatis* Cuvier, 1816

577 *Myliobatis* sp.

578 (Fig. 20)

579

580 **Referred specimens:** n = 30: ASIZF0100581–0100589, CMM F0378, F0379, F0381, F0383–
581 F0387, F0389–F0393, F0394, F0396–F0398, F0410, F0411, F2855, NTM I01118.

582 **Description:** Each tooth of *Myliobatis* has a flat occlusal surface and is laterally elongated and
583 hexagonal that may be straight or slightly arched. The root is polyaulocorhizous with well-
584 defined anteroposteriorly oriented, vertical lamellar plates separated by deep grooves, where the
585 crown overhangs the root on the labial (anterior) face. The lingual and labial faces are
586 ornamented with a network of fine reticulated ridges that grade into longitudinal ridges in the
587 apical and become finer and anastomotic.

588 **Remarks:** The tooth plates of *Myliobatis* are similar to those of *Aetomylaeus* and *Aetobatus*, but
589 the lateral angle of the hexagonal tooth plates in *Aetomylaeus* is more oblique than that of
590 *Myliobatis* (Ebersole, Cicimurri & Stringer, 2019). The vertical lamellar plates of the root in
591 *Myliobatis* are coarser than *Aetobatus*. Teeth of *Myliobatis* lack the tuberculated enameloid on
592 the occlusal surface, whereas teeth of *Aetomylaeus* are reticulated on the labial and lingual faces
593 (Ebersole, Cicimurri & Stringer, 2019). Because the total morphological variation range of teeth
594 in many of the aetobatid and myliobatid (Myliobatinae) species is unknown (e.g., see Hovestadt
595 & Hovestadt-Euler, 2013), we refrain from assigning the *Aetobatus* (see above) and *Myliobatis*
596 teeth described here to the species level.

597

598

599 **Discussion**

600 Previous works on fossil elasmobranchs in Taiwan are very scarce, where they were limited in
601 scope, often lacked formal description, and were mostly not based on specimens in museum
602 repositories (Lin et al., 2021). Huang (1965) reported three shark taxa while describing a fossil
603 whale tympanic bone from the early Pleistocene Cholan Formation in northern Taiwan (as early
604 Pliocene in Huang, 1965). Although the whereabouts of the specimens is unknown, it is one of
605 the earliest accounts reporting fossil shark teeth in Taiwan. Uyeno (1978) listed nine
606 elasmobranch taxa from the Pleistocene Chochen–Tsailiao area with images of the specimens but
607 without descriptions, and these materials are reviewed in this present study.

608

609 Perhaps the most complete description on a single fossil shark assemblage in Taiwan is the one
610 by Tao & Hu (2008) from the late Miocene Tangenshan Sandstone Formation in Chiahsien
611 County, Kaohsiung. They described five taxa common in late Miocene marine deposits (*Otodus*
612 *megalodon*, *Odontaspis* sp., †*Isurus hastalis*, †*Hemipristis serra*, and *Carcharhinus* sp.) as well
613 as a new extinct species of *Hemipristis*, *H. liui* Tao & Hu, 2008. The specimen of *H. liui* is an
614 upper tooth and is characterized by asymmetric serrations on the distal and mesial cutting edges.
615 The occurrences of *Otodus megalodon* are sparsely recorded from Taiwan (Hu & Tao, 1993; Tao
616 & Hu, 2008) and are mostly present in private collections, which are potentially one of the
617 directions for future research efforts (Haug et al., 2020; Lin et al., 2021).

618

619 The materials were mainly based on surface collecting that spanned over more than three
620 decades, and we note that our bulk sediment samples (830 kg, see methods) only yielded three
621 specimens (ASIZF0100548, ASIZF0100590, and ASIZF0100591). Surface collecting likely
622 results in sampling bias towards larger specimens underrepresenting smaller specimens (Welton
623 & Farish, 1993; Perez, 2022). Nevertheless, 697 elasmobranch teeth from the Liuchungchi
624 Formation in Niubu described in this study reveal the presence of at least 20 elasmobranch taxa
625 (Table 1). The excellent overall preservation allowed species-level taxonomic identification for
626 most of the specimens, which in turn, permitted the elucidation of the diverse elasmobranch
627 community. In fact, the assemblage represents the most diverse elasmobranch paleofauna from
628 Taiwan reported to date. Moreover, the species richness and diversity indices suggest that our
629 assemblage is highly diverse even with respect to other contemporaneous assemblages from
630 temperate and tropical West Pacific (Table 2, Supplemental Table S1). Together, the high
631 diversity captured in our study is significant in the spatio-temporal context.

632

633 The abundant and large teeth of *Carcharodon carcharias* are remarkable. *Carcharodon*
634 *carcharias* is distributed along southern, eastern, and northeastern Taiwan today, but not on the
635 west coast where the fossils are found (Teng, 1958; Shen, 1993; Ebert et al., 2013; Shao, 2022).
636 According to the Fisheries Agency, Council of Agriculture, Taiwan (Taiwan Fisheries Agency,

637 2021), a total of 39 individuals of *C. carcharias* were caught between 2012 and 2021, with the
638 majority of landings being in northeastern Taiwan. However, at our fossil sites, teeth of *C.*
639 *carcharias* are the second most abundant remains (n = 55) among specimens identified to the
640 species level in this study, next to teeth of *Carcharhinus leucas* (n = 71, Table 1). Of the 55
641 isolated teeth that are interpreted to have most certainly come from 55 different individuals, 44
642 of them are well-preserved, offering their tooth position identifications and crown heights (CH).
643 Based on the linear regression equation between the CH and fish total length (TL) for each tooth
644 position in extant *Carcharodon carcharias* presented by Shimada (2003), the CH of each of the
645 44 teeth was used to estimate the TL of each fossil individual (Supplemental Table S2). Our
646 specimens are normally distributed (Shapiro–Wilk test = 0.853, p = 0.08) and range in fish
647 length from 1.9 to 5.6 m, with a mean of 3.5 m (Supplemental Table S2), suggesting presence of
648 many mature, large individuals (Ebert et al., 2013).

649

650 One of the most noteworthy occurrences reported in this study is that of the extinct species
651 †*Hemipristis serra*. The species is known worldwide, but most of the documented occurrences
652 are from the Miocene and Pliocene deposits (e.g., Yabumoto & Uyeno, 1994; Sánchez-Villagra
653 et al., 2000; Marsili et al., 2007; Portell et al., 2008; Visaggi & Godfrey, 2010; Carrillo-Briceño
654 et al., 2015; Kocsis et al., 2019). The fossil record indicates that the fossil species preferred
655 warm neritic environments (Cappetta, 2004, 2012). Although most previous studies suggest its
656 last appearance at the end of the Pliocene, new evidence indicates that †*H. serra* persisted into
657 the Pleistocene in North America (Ebersole, Ebersole & Cicimurri, 2017; Boessenecker,
658 Boessenecker & Geisler, 2018; Perez, 2022). Teeth of *Hemipristis* that may belong to *H. serra*
659 have been reported from Pleistocene and ‘Plio-Pleistocene’ deposits in Sulawesi and Java,
660 Indonesia (*H. cf. serra* by Hooijer, 1954, 1958; simply “*Hemipristis*” by Yudha et al., 2018).
661 Previous records of †*H. serra* from Taiwan were reported by Uyeno (1978) from an uncertain
662 stratigraphic horizon along Tsailiao River, and that by Tao & Hu (2008) from the Miocene
663 Kueichulin Formation in southern Taiwan. The †*H. serra* specimens described here are the first
664 confirmed Pleistocene record in Taiwan, and along with the putative Indonesian records
665 (Hooijer, 1954, 1958; Yudha et al., 2018), the geologically youngest records of the extinct
666 species in the Northwest Pacific, meaning that the North American occurrences were not
667 isolated. It should be noted that the preservation of all specimens of †*H. serra* described in this
668 study are excellent (Fig. 6), and thus they most certainly do not represent fossils derived from an
669 older horizon.

670

671 The assemblage is dominated by two genera, *Carcharhinus* (Carcharhinidae, n = 462) and
672 *Carcharodon* (Lamidae, n = 52), comprising more than 77.5% of the total specimen count and
673 about half of the taxa identified (11 out of 20). From a paleoecological perspective, the
674 composition is roughly similar to the one found in modern western Taiwan (Ebert et al., 2013;
675 Shao, 2022). For example, the most abundant species of *Carcharhinus* in this study, *C. leucas*,
676 presently lives close to the coastal area of tropical and subtropical riverine and lacustrine

677 (Compagno, 1984). The second-most abundant species in this study, *Carcharodon carcharias*,
678 inhabits inshore shallow water to open ocean and, as a top predator, feeds on larger marine
679 mammals and fishes (Ebert et al., 2013; Compagno, 2002). While pelagic sharks *Carcharhinus*
680 *plumbeus* and *C. longimanus* are also frequently represented in the Pleistocene assemblage, the
681 occurrences of *C. altimus*, *Aetobatus* sp., and *Myliobatis* sp. may suggest the possible presence
682 of deeper sandy, flat bottoms (Compagno, 1984). The abundant associated marine vertebrate
683 fossils, including teleost bones (Tao, 1993), otoliths (Lin et al., 2018), and whale bones (Xue,
684 2004), indicate a rich, thriving marine ecosystem in the area. The sedimentary environment of
685 the Liuchungchi Formation further points to shoreface to inner offshore setting, with several
686 transgressive and regressive cycles (Chen, 2016). Taken together, the coastal areas in southwest
687 Taiwan during the early Pleistocene can be interpreted as an inshore to offshore shallow-water
688 environment with sandy bottoms.

689

690 **Conclusions**

691 Fossil elasmobranch fauna from the tropical-subtropical West Pacific is poorly known compared
692 to its modern analog, impeding our understanding of the formation of this current marine
693 biodiversity hotspot. Using elasmobranch fossils from an early Pleistocene locality in southern
694 Taiwan, we report a previously unreported but highly diverse shark and ray fauna from the
695 region. The taxonomic composition of the assemblage reveals a nearshore shallow-water
696 paleoenvironment and supports the sedimentary interpretation. In addition, the presence of
697 *†Hemipristis serra* and large specimens of *Carcharodon carcharias* highlight the potential for
698 similar studies from other strata and localities, which would allow a more comprehensive picture
699 of the evolutionary history and biogeographic distribution of the species. The present study can
700 be regarded as the most extensive on elasmobranch fossils from Taiwan.

701

702 **Acknowledgements**

703 We would like to express our sincere gratitude to Prof. Hsi-Jen Tao (National Taiwan
704 University) who donated the specimens to the Biodiversity Research Museum, Academia Sinica,
705 Taiwan. We also thank Mrs. Hsiao I-Ju (Chiayi Municipal Museum, CMM) for her
706 administrative assistance in examining the CMM collection, and Miss Sun You-Yu (National
707 Taiwan Museum) for accessing the collection described by Uyeno (1978). This manuscript has
708 been improved based on constructive reviews by Kenneth De Baets, Dana Ehret, Laszlo Kocsis,
709 and an anonymous reviewer.

710

711 **References**

712 Agassiz L. 1833–1843. *Recherches sur les poissons fossiles: une introduction à l'étude de ces*
713 *animaux*. Neuchatel, Switzerland: Imprimerie de Petitpierre.

714 Agassiz L. 1858. A new species of skate from the Sandwich Islands. *Proceedings of the Boston*
715 *Society of Natural History* 6 (1856–1859):385.

716 Bellwood DR, Meyer CP. 2009. Searching for heat in a marine biodiversity hotspot. *Journal of*
717 *Biogeography* 36:569–576 DOI: 10.1111/j.1365-2699.2008.02029.x.

718 Berg LS. 1958. *System der rezenten und fossilen fischartigen und fische*. Berlin: Deutsche Verlag
719 Wissenschaften.

720 Blainville HMD de. 1816. Prodrome d'une nouvelle distribution systematique de regne animal.
721 *Bulletin de Sciences de la Société Philomatique de Paris* 8:113–124.

722 Bleeker P. 1852. Bijdrage tot de kennis der Plagiostomen van den Indischen Archipel.
723 *Verhandelingen van het Bataviaasch Genootschap van Kunsten en Wetenschappen* 24:1–
724 92.

725 Bleeker P. 1854. Faunae ichthyologicae japonicae species novae. *Natuurkundig Tijdschrift voor*
726 *Nederlandsch Indië* 6:395–426.

727 Boessenecker SJ, Boessenecker RW, Geisler JH. 2018. Youngest record of the extinct walrus
728 *Ontocetus emmonsi* from the Early Pleistocene of South Carolina and a review of North
729 Atlantic walrus biochronology. *Acta Palaeontologica Polonica* 63:279–286 DOI:
730 10.4202/app.00454.2018.

731 Bonaparte CL. 1835. Prodromus systematis ichthyologiae. *Nuovi Annali delle Scienze naturali Bologna (Ser. 1) (ann. 2)* 4:181–196, 272–277.

732 Bonaparte CL. 1840. *Iconografia della fauna italica per le quattro classi degli animali*
733 *vertebrati. Tomo III*. Roma: Dalla Tipografia Salviucci.

734 Buckeridge JS, Chan BKK, Lee S-W. 2018. Accumulations of fossils of the whale barnacle
735 *Coronula bifida* Bronn, 1831 (Thoracica: coronulidae) provides evidence of a Late
736 Pliocene cetacean migration route through the Straits of Taiwan. *Zoological Studies* 57:1–
737 12.

738 Cappetta H. 2004. *Handbook of Paleoichthyology, Vol. 3B: Chondrichthyes II Mesozoic and*
739 *Cenozoic Elasmobranchii*. München: Verlag Dr Friedrich Pfeil.

740 Cappetta H. 2012. *Handbook of Paleoichthyology, Vol. 3E: Chondrichthyes Mesozoic and*
741 *Cenozoic Elasmobranchii: Teeth*. München: Verlag Dr Friedrich Pfeil.

742 Carrillo-Briceño JD, De Gracia C, Pimiento C, Aguilera OA, Kindlimann R, Santamarina P,
743 Jaramillo C. 2015. A new Late Miocene chondrichthyan assemblage from the Chagres
744 Formation, Panama. *Journal of South American Earth Sciences* 60:56–70 DOI:
745 10.1016/j.jsames.2015.02.001

746 Chen W-S. 2016. *An introduction to the geology of Taiwan*. Taipei: Geological Society of
747 Taiwan.

748 Chen W-S, Huang N-E, Yang C-C. 2011. Pleistocene sequence stratigraphic characteristics and
749 foreland basin evolution, southwestern Taiwan. *Special Publication of the Central*
750 *Geological Survey* 25:1–38.

751 Chou J-T. 1975. A sedimentologic study of the Miocene Pachangchi Sandstone in the Chiayi
752 region, Western Taiwan. *Petroleum Geology of Taiwan* 12:81–96.

753 Cigala-Fulgori F, Mori D. 1979. Osservazioni tassonomiche sul genere Galeocerdo (Selachii,
754 Carcharhinidae) con particolare riferimento a Galeocerdo cuvieri (Peron & Lesueur) nel
755 Pliocene del Mediterraneo. *Bollettino della Società Paleontologica Italiana* 18:117–132.

756 Compagno LJV. 1973. Interrelationships of living elasmobranchs. *Zoological Journal of the*
757 *Linnean Society* 53:15–61.

758 Compagno LJV. 1984. *FAO species catalogue. Sharks of the world: An annotated and illustrated*
759 *catalogue of shark species known to date, Volume 4: Carcharhiniformes*. Rome: Food and
760 Agriculture Organization of the United Nations.

761 Compagno LJV. 1988. *Sharks of the order Carcharhiniformes*. New Jersey: Princeton University
762 Press.

763 Compagno, LJV. 2002. *FAO species catalogue. Sharks of the world: An annotated and*
764 *illustrated catalogue of shark species known to date, Volume 2: Bullhead, mackerel and*
765 *carpet sharks (Heterodontiformes, Lamniformes and Orectolobiformes)*. Rome: Food and
766 Agriculture Organization of the United Nations.

767 Covey M. 1984. Lithofacies analysis and basin reconstruction, Plio-Pleistocene western Taiwan
768 foredeep. *Petroleum Geology of Taiwan* 20:53–83.

769 Cuvier GLFCD. 1816. Le Règne Animal distribué d'après son organization, pour servir de base à
770 l'histoire naturelle des animaux et d'introduction à l'anatomie comparée. *Les reptiles, les*
771 *poissons, les mollusques et les annéllides*. Paris, 4 Vols, Edition 1. Poissons 2:104–351.

772 Ebersole JA, Ebersole SM, Cicimurri DJ. 2017. The occurrence of early Pleistocene marine fish
773 remains from the Gulf Coast of Mobile County, Alabama, USA. *Palaeodiversity*
774 10:97–115 DOI: 10.18476/pale.v10.a6.

775 Ebersole JA, Cicimurri DJ, Stringer GL. 2019. Taxonomy and biostratigraphy of the
776 elasmobranchs and bony fishes (Chondrichthyes and Osteichthyes) of the lower-to-middle
777 Eocene (Ypresian to Bartonian) Claiborne Group in Alabama, USA, including an analysis
778 of otoliths. *European Journal of Taxonomy* 585:1–274.

779 Ebert DA, White WT, Ho H-C, Last PR, Nakaya K, Séret B, Straube N, Naylor GJP, De
780 Carvalho MR. 2013. An annotated checklist of the chondrichthians of Taiwan. *Zootaxa*
781 3752:279–386

782 Ebert DA, Dando M, Fowler S. 2021. *Shark of the world, A complete guide*. New Jersey:
783 Princeton University Press.

784 Ehret DJ, MacFadden BJ, Jones DS, Devries TJ, Foster DA, Salas-Gismondi R. 2012.
785 Origin of the white shark *Carcharodon* (Lamniformes: Lamnidae) based on
786 recalibration of the Upper Neogene Pisco Formation of Peru. *Palaeontology* 55:1139–
787 1153 DOI: 10.1111/j.1475-4983.2012.01201.x.

788 Fricke R, Eschmeyer WN, Van der Laan R, eds. 2022. Eschmeyer's catalog of fishes: genera,
789 species, references, version 02/2022, Available at
790 <http://researcharchive.calacademy.org/research/ichthyology/catalog/fishcatmain.asp>
791 (accessed May 2022).

792 Froese R, Pauly D, eds. 2022. FishBase. World Wide Web electronic publication.
793 www.fishbase.org, version 02/2022, Available at <https://www.fishbase.se/search.php>
794 (accessed July 2022).

795 Garrick JAF. 1982. Sharks of the genus *Carcharhinus*. NOAA Technical Report NMFS Circular
796 445, Seattle, Washington: NMFS Scientific Publications Office.

797 Griffith E, Smith CH. 1834. The class Pisces, arranged by the Baron Cuvier, with supplementary
798 additions, by Edward Griffith, F.R.S., &c. and Lieut.-Col. Charles Hamilton Smith, C. H.,
799 K. W., F. R., L. S. S., &c. &c. In: Cuvier G, ed. *The animal kingdom arranged in*
800 *conformity with its organization, with additional descriptions of all the species hitherto*
801 *named, and of many not before noticed, by Edward Griffith, and others.* London: Whittaker
802 & Co.

803 Hasse JCF. 1878. Das natürliche System des Elasmobranchier auf Grundlage des Baues und der
804 Entwicklung des Wirbelsäule. *Zoologischer Anzeiger* 1:144–148, 167–172, 7:144–148,
805 8:167–172.

806 Haug C, Reumer JWF, Haug JT, et al. 2020. Comment on the letter of the Society of Vertebrate
807 Paleontology (SVP) dated April 21, 2020 regarding “Fossils from conflict zones and
808 reproducibility of fossil-based scientific data”: the importance of private collections.
809 *Paläontologische Zeitschrift* 94:413–429 DOI: 10.1007/s12542-020-00522-x.

810 Herman J, Hovestadt-Euler M, Hovestadt DC. 1998. Contributions to the study of the
811 comparative morphology of teeth and other relevant ichthyodorulites in living
812 supraspecific taxa of Chondrichthyan fishes. Part B: Batomorphii 4a: Order Rajiformes –
813 Suborder Myliobatoidei – Superfamily Dasyatoidea – Family Dasyatidae – Subfamily
814 Dasyatinae – Genera: *Amphotistius*, *Dasyatis*, *Himantura*, *Pastinachus*, *Pteroplatytrygon*,
815 *Taeniura*, *Urogymnus* and *Urolophoides* (incl. supraspecific taxa of uncertain status and
816 validity), Superfamily Myliobatoidea – Family Gymnuridae – Genera: *Aetoplatea* and
817 *Gymnura*, Superfamily Plesiobatoidea – Family Hexatrygonidae – Genus: *Hexatrygon*.
818 *Bulletin de l'Institut Royal des Sciences Naturelles de Belgique, Biologie* 68:145–197.

819 Herman J, Hovestadt-Euler M, Hovestadt DC. 1999. Contributions to the study of the
820 comparative morphology of teeth and other relevant ichthyodorulites in living
821 supraspecific taxa of Chondrichthyan fishes. Part B: Batomorphii 4b: Order Rajiformes –
822 Suborder Myliobatoidei – Superfamily Dasyatoidea – Family Dasyatidae – Subfamily
823 Dasyatinae – Genera: *Taeniura*, *Urogymnus*, *Urolophoides* – Subfamily
824 Potamotrygoninae – Genera: *Disceus*, *Plesiotrygon*, and *Potamotrygon* (incl. supraspecific
825 taxa of uncertain status and validity), Family Urolophidae – Genera: *Trygonoptem*,
826 *Urolophus* and *Urotrygon* – Superfamily Myliobatidea – Family: Gymnuridae – Genus:
827 *Aetoplatea*. *Bulletin de l'Institut Royal des Sciences Naturelles de Belgique, Biologie*
828 69:161–200.

829 Herman J, Hovestadt-Euler M, Hovestadt DC. 2000. Contributions to the study of the
830 comparative morphology of teeth and other relevant ichthyodorulites in living
831 supraspecific taxa of Chondrichthyan fishes. Part B: Batomorphii 4c: Order Rajiformes –
832 Suborder Myliobatoidei – Superfamily Dasyatoidea – Family Dasyatidae – Subfamily
833 Dasyatinae – Genus: *Urobatis*, Subfamily Potamotrygoninae – Genus: *Paratrygon*,
834 Superfamily Plesiobatoidea – Family Plesiobatidae – Genus: *Plesiobatis*, Superfamily
835 Myliobatoidea – Family Myliobatidae - Subfamily Myliobatinae – Genera : *Aetobatus*,
836 *Aetomylaeus*, *Myliobatis* and *Pteromylaeus*, Subfamily Rhinopterinae – Genus: *Rhinoptera*
837 and Subfamily Mobulinae – Genera: *Manta* and *Mobula*. Addendum 1 to 4a: erratum to
838 Genus *Pteroplatytrygon*. *Bulletin de l'Institut Royal des Sciences Naturelles de Belgique, Biologie*
839 70:5–67.

840 Ho C-S. 1967. Foothill tectonics of Taiwan. *Bulletin of the Geological Survey of Taiwan* 25:9–

841 28.

842 Ho C-S. 1976. Structural evolution of Taiwan, *Tectonophysics* 4:367–378.

843 Hooijer D. 1954. Pleistocene vertebrates from Celebes. IX. Elasmobranchii. X. Testudinata.

844 *Proceedings of the Koninklijke Nederlandse Akademie van Wetenschappen, Series B*,
845 57:475–789.

846 Hooijer DA. 1958. The Pleistocene vertebrate fauna of Celebes. *Asian Perspectives* 2(2):71–76.

847 Hovestadt DC, Hovestadt-Euler M. 2013. Generic assessment and reallocation of Cenozoic
848 Myliobatinae based on new information of tooth, tooth plate and caudal spine morphology
849 of extant taxa. *Palaeontos* 24:1–66.

850 Hu C-H. 1989. Manual for ten geological routes in central Taiwan—route 7: geology along the
851 Nanheng Highway—Tsailiao, Peiliao, Chiahsien. In: Faculty members of the Department
852 of Earth Sciences, National Taiwan Normal University, editors. *Field manual of the*
853 *geology of Taiwan (II)*. Taipei: Department of Earth Sciences, National Taiwan Normal
854 University, 105–163.

855 Hu C-H, Tao H-J. 1993. *The fossil faunas of Penghu Islands, Taiwan*. Penghu: Penghu District
856 Cultural Center Publications.

857 Hu C-H, Tao H-J. 1996. *Crustacean fossils of Taiwan*. Taipei: San Min Book.

858 Hu C-H, Tao H-J. 2004. Studies on the Neogene crabs from south-western foothills of Taiwan.
859 *Acta Palaeontologica Sinica* 43(4):537–555.

860 Huang T. 1965. A new species of a whale tympanic bone from Taiwan, China. *Transaction and*
861 *Proceedings of the Palaeontological Society of Japan* 61:183–187.

862 Huang W-C. 2010. Stratigraphic sequences in distal part of foreland Basin in Southwestern
863 Taiwan: Model of interplay between tectonics and eustasy. Master Thesis, Department of
864 Earth Sciences, National Cheng Kung University.

865 Hubbell G. 1996. *Using tooth structure to determine the evolutionary history of the white shark*.
866 *In Great white sharks: the biology of Carcharodon Carcharias*. San Diego: Academic
867 Press.

868 Huxley TH. 1880. On the application of the laws of evolution to the arrangement of the
869 Vertebrata, and more particularly of the Mammalia. *Proceedings of the Zoological Society*
870 *of London* 43:649–662.

871 Jordan DS, Gilbert CH. 1879. Notes on the fishes of Beaufort Harbor, North Carolina.
872 *Proceedings of the United States National Museum* 55:365–388.

873 Jordan DS, Evermann BW. 1896. The fishes of North and Middle America. *Bulletin of the*
874 *United States National Museum* 47:1–1240.

875 Kajiura SM, Tricas T. 1996. Seasonal dynamics of dental dimorphism in the Atlantic Stingray
876 *Dasyatis sabina*. *Journal of Experimental Biology* 199:2297–306.

877 Karasawa H. 1989. Late Cenozoic elasmobranchs from the Hokuriku district, central Japan. *The*
878 *science reports of the Kanazawa University* 34(1):1–57.

879 Kawase M, Nishimatsu K. 2016. Elasmobranch remains from the Middle Pleistocene Takamatsu

880 Silty Sandstone of the Toyohashi Formation, the Atsumi Group, Aichi Prefecture, Central
881 Japan. *Bulletin of the Mizunami Fossil Museum* 42:47–61.

882 Kocsis L, Razak H, Briguglio A, Szabó M. 2019. First report on a diverse Neogene fossil
883 cartilaginous fish fauna from Borneo (Ambig Hill, Brunei Darussalam). *Journal of*
884 *Systematic Palaeontology* 17(10):791–819 DOI: 10.1080/14772019.2018.1468830.

885 Koumans FP. 1949. On some fossil fish remains from Java. *Zoologische Mededelingen*
886 30(5):77–82.

887 Last, PR, Naylor GJP, Manjaji-Matsumoto BM. 2016. A revised classification of the family
888 Dasyatidae (Chondrichthyes: Myliobatiformes) based on new morphological and
889 molecular insights. *Zootaxa* 4139:345–368.

890 Lesueur CA. 1818. Description of several new species of North American fishes. *Journal of the*
891 *Philadelphia Academy of Natural Sciences* 1:222–235.

892 Lin A-T, Watts AB. 2002. Origin of the west Taiwan basin by orogenic loading and flexure of a
893 rifted continental margin. *Journal of Geophysical Research* 107:2185.

894 Lin C-H, Chien C-W. 2022. Late Miocene otoliths from northern Taiwan: insights into the rarely
895 known Neogene coastal fish community of the subtropical northwest Pacific. *Historical*
896 *Biology* 34:361–382 DOI: 10.1080/08912963.2021.1916012

897 Lin C-H, Chien C-W, Lee S-W, Chang C-W. 2021. Fossil fishes of Taiwan, a review and
898 prospectation. *Historical Biology* 33:1362–1372 DOI: 10.1080/08912963.2019.1698563.

899 Lin C-H, Ou H-Y, Lin C-Y, Chen H-M. 2022. First skeletal fossil record of the red
900 seabream *Pagrus major* (Sparidae, Perciformes) from the Late Pleistocene of subtropical
901 West Pacific, southern Taiwan. *Zoological Studies* 61:10 DOI: 10.6620/ZS.2022.61-10.

902 Lin C-H, Wang L-C, Wang C-H, Chang C-W. 2018. Common early Pleistocene fish otoliths
903 from Niubu in Chia-Yi County, southwestern Taiwan. *Journal of the National Taiwan*
904 *Museum* 71:47–68 DOI: 10.6532/JNTM.201809_71(3).04.

905 Linnaeus C. 1758. *Systema naturae per regna tria naturae, secundum classes, ordines, genera,*
906 *species, cum characteribus, differentiis, synonymis, locis, vol. I.* Stockholm: Laurentii
907 Salvii.

908 Lundberg N, Reed DL, Liu C-S, Lieske J. 1997. Forearc-basin closure and arc accretion in the
909 submarine suture zone south of Taiwan. *Tectonophysics* 274:5–23.

910 Marsili S, 2006. Revision of the teeth of the genus *Carcharhinus* (Elasmobranchii;
911 Carcharhinidae) from the Pliocene of Tuscany, Italy. *Rivista Italiana di Paleontologia e*
912 *Stratigrafia* 113:79–95 DOI: 10.13130/2039-4942/6360.

913 Marsili S, Carnevale G, Danese E, Bianucci G, Landini W. 2007. Early Miocene vertebrates
914 from Montagna della Maiella, Italy. *Annales de Paléontologie* 93:1, 27–66 DOI:
915 10.1016/j.anpal.2007.01.001.

916 Müller J, Henle FGJ. 1837. *Gattungen der Haifische und Rochen nach einer vom ihm mit Hrn*
917 *Henle unternommenen gemeinschaftlichen Arbeit über die Naturgeschichte der*
918 *Knorpelfische.* Berlin: Berichte der königlich preussischen Akademie der Wissenschaften.

919 Müller J, Henle FGJ. 1838. On the generic characters of cartilaginous fishes. *Magazine of*

920 *Natural History* 2:33–91.

921 Müller J, Henle J. 1839. *Systematische Beschreibung der Plagiostomen*. Berlin: Verlag von veit
922 und comp.

923 Myers N, Mittermeier RA, Mittermeier CG, da Fonseca GAB, Kent J. 2000. Biodiversity
924 hotspots for conservation priorities. *Nature* 403:853–858.

925 Nagel S, Castelltort S, Wetzel A, Willett SD, Mouthereau F, Lin A-T. 2013. Sedimentology and
926 foreland basin paleogeography during Taiwan arc continent collision. *Journal of Asian*
927 *Earth Sciences* 62:180–204.

928 Nardo GD. 1827. Prodromus observationum et disquisitionum Adriaticae ichthyologiae.
929 *Giornale di fisica, chimica e storia naturale, medicina, ed arti* 10:22–40.

930 Naylor GJP, Marcus LF. 1994. Identifying isolated shark teeth of the genus *Carcharhinus* to
931 species relevance for tracking phyletic change through the fossil record. *American Museum*
932 *Novitates* 3109:56.

933 Nelson JS, Grande TC, Wilson MVH. 2016. *Fishes of the world*. New Jersey: John Wiley &
934 Sons.Perez VJ. 2022. The chondrichthyan fossil record of the Florida Platform
935 (Eocene–Pleistocene). *Paleobiology*, 1–33 DOI: 10.1017/pab.2021.47.

936 Pérón F, Lesueur CA. 1822. Description of a *Squalus*, of a very large size, which was taken
937 on the coast of New Jersey. *Journal of the Philadelphia Academy of Natural Sciences*
938 2:343–352.

939 Poey F. 1861. Conspectus piscium cubensium. In: *Memorias sobre la historia natural de la*
940 *Isla de Cuba, acompañadas de sumarios Latinos y extractos en Francés*. Barcina, La
941 Habana: ealle de la Reina, 337–442.

942 Portell RW, Hubbell G, Donovan SK, Green JL, Harper DAT, Pickerill R. 2008. Miocene
943 sharks in the Kendeace and Grand Bay formations of Carriacou, The Grenadines,
944 Lesser Antilles. *Caribbean Journal of Science* 44:279–286 DOI:
945 10.18475/cjos.v44i3.a2.

946 Purdy RW, Schneider VP, Applegate SP, McLellan JH, Meyer RL, Slaughter BH. 2001. The
947 Neogene sharks, rays, and bony fishes from Lee Creek Mine, Aurora, North Carolina.
948 In Ray CE, Bohaska DH, eds. *Geology and Paleontology of the Lee Creek Mine,*
949 *North Carolina, III: Smithsonian Contributions to Paleobiology*. Washington:
950 Smithsonian Institution Press, 71–160.

951 Purdy RW. 2006. A key to common genera of Neogene shark teeth. Available at
952 <http://paleobiology.si.edu/pdfs/sharktoothKey.pdf> (accessed May 2022).

953 Rafinesque CS. 1810. *Caratteri di alcuni nuovi generi e nuove specie di animali e piante*
954 *della Sicilia, con varie osservazioni sopra i medisimi*. Palermo, Italy: Sanfilippo.

955 Ribas-Deulofeu L, Wang Y-C, Lin C-H. 2021. First record of Late Miocene *Dendrophyllia*
956 de Blainville, 1830 (Scleractinia: Dendrophylliidae) in Taiwan. *Terrestrial,*
957 *Atmospheric and Oceanic Sciences* 32:1061–1068 DOI: 10.3319/TAO.2021.09.13.02.

958 Rüppell WPES. 1837. *Neue Wirbelthiere zu der Fauna von Abyssinien gehörig entdeckt und*

959 *beschrieben von Dr. Eduard Ruppell.* Frankfurt am Main: Fische des Rothen Meeres,
960 Siegmund Schmerber.

961 Sánchez-Villagra MR, Burnham RJ, Campbell DC, Feldmann RM, Gaffney ES, Kay RF,
962 Lozsan R, Purdy R, Thewissen JGM. 2000. A new near-shore marine fauna and flora
963 from the Early Neogene of northwestern Venezuela. *Journal of Paleontology* 74:957–
964 968 DOI:10.1017/s0022336000033126.

965 Shao K-T. 2022. Taiwan Fish Database. WWW Web electronic publication. Available at
966 <http://fishdb.sinica.edu.tw> (accessed July 2022).

967 Shen S-C. 1993. *Fishes of Taiwan*. Taipei: Department of Zoology, National Taiwan
968 University.

969 Shimada K. 2002. Dental homologies in lamniform sharks (Chondrichthyes: Elasmobranchii).
970 *Journal of Morphology* 251:38–72.

971 Shimada K. 2003 (date of imprint 2002). The relationship between the tooth size and total body
972 length in the white shark, *Carcharodon carcharias*. *Journal of Fossil Research* 35:28–33.

973 Smith A. 1938. In: Müller J, Henle FGJ, eds. On the generic characters of cartilaginous fishes,
974 with descriptions of new genera. *Magazine of Natural History* 2:33–37, 88–91.

975 Smith JLB. 1957. The rare shark *Hemipristis elongatus* (Klunzinger), 1871, from Zanzibar and
976 Mozambique. *Annals and Magazine of Natural History* 10:555–560 DOI:
977 10.1080/00222935708655997.

978 Springer S. 1950. A revision of North American sharks allied to the Genus *Carcharhinus*.
979 *American Museum Novitates* 1451:1–13.

980 Stach LW. 1957. Stratigraphic subdivision and correlation of the upper Cenozoic sequence in the
981 foothills region east of Chiayi and Hsinying, Taiwan, China. *Symposium on Petroleum
982 Geology of Taiwan*, 177–230.

983 Suppe J. 1984. Kinematics of arc-continent collision, flipping of subduction, and back-arc
984 spreading near Taiwan. *Journal of the Geological Society of China* 6:21–33.

985 Taiwan Fisheries Agency. 2021. Coastal great white sharks, megamouth sharks, elephant sharks,
986 manta rays reported statistics. Fisheries Agency, Taipei, Taiwan.

987 Tanaka T, Taru H. 2022. Fossil elasmobranchs from the Iimuro Formation, Kazusa Group,
988 Lower Pleistocene, Komae City, Tokyo, Japan. *Natural History Report of Kanagawa*
989 43:147–156 DOI: 10.32225/nkpmnh.2022.43_147.

990 Taniuchi T, Shimizu M. 1993. Dental sexual dimorphism and food habits in the stingray
991 *Dasyatis akajei* from Tokyo Bay, Japan. *Nippon Suisan Gakkaishi* 59:53–60.

992 Tao H-J. 1993. A new Miocene fossil species *Priacanthus liui* (Pisces: perciformes) from the
993 Nanchung Formation in Chiayi Hsien, Taiwan. *Bulletin of the National Museum of Nature
994 and Science* 4:91–100.

995 Tao H-J, Hu C-H. 2008. Fossil chondrichthyes fishes of Chia-hsien, Kaoshung County, Taiwan.
996 *Journal of the National Taiwan Museum* 61:41–62.

997 Teng H-T. 1958. Studies on the elasmobranch fishes from Formosa. Part 1. Eighteen unrecorded

998 species of sharks from Formosa. *Reports of the Laboratory of Fishery Biology, Taiwan*
999 *Fisheries Research Institute* 3:1–30.

1000 Teng L-S. 1990. Geotectonic evolution of late Cenozoic arc-continent collision in Taiwan.
1001 *Tectonophysics* 183:57–76.

1002 Türtscher J, López-Romero FA, Jambura PL, Kindlimann R, Ward DJ, Kriwet J. 2021.
1003 Evolution, diversity, and disparity of the tiger shark lineage *Galeocerdo* in deep time.
1004 *Paleobiology* 47:574–590 DOI: 10.1017/pab.2021.6.

1005 Uyeno T. 1978. A preliminary report on fossil fishes from Ts'o-chen Tainan. *Science Report*
1006 *Geology and Paleontology* 1:5–17.

1007 Valenciennes A. 1839. In: Müller J, Henle FGJ, eds. *Systematische Beschreibung der*
1008 *Plagiostomen*, vol. 2. Berlin: Verlag von veit und comp, 39–102.

1009 Visaggi CC, Godfrey SJ. 2010. Variation in composition and abundance of Miocene shark teeth
1010 from Calvert Cliffs, Maryland. *Journal of Vertebrate Paleontology* 30:26–35 DOI:
1011 10.1080/02724630903409063.

1012 Voigt M, Weber D. 2011. *Field guide for sharks of the genus Carcharhinus*. München:
1013 Verlag Dr. Friedrich Pfeil.

1014 Weigmann S. 2016. Annotated checklist of the living sharks, batoids and chimaeras
1015 (Chondrichthyes) of the world, with a focus on biogeographical diversity. *Journal of*
1016 *Fish Biology* 88:837–1037 DOI: 10.1111/jfb.12874.

1017 Welton BJ, Farish RF. 1993. *The collector's guide to Fossil Sharks and Rays from the*
1018 *Cretaceous of Texas*. Lewisville, Texas: Before Time.

1019 White WT. 2012. A redescription of *Carcharhinus dussumieri* and *C. sealei*, with resurrection of
1020 *C. coatesi* and *C. tjutjot* as valid species (Chondrichthyes: Carcharhinidae). *Zootaxa*
1021 3241:1–34.

1022 White WT, Kawauchi J, Corrigan S, Naylor G. 2015. Redescription of the eagle rays *Myliobatis*
1023 *hamlynii* Ogilby, 1911 and *M. tobijei* Bleeker, 1854 (Myliobatiformes: Myliobatidae) from
1024 the East Indo-West Pacific. *Zootaxa* 3948(3):521–548 DOI: 10.11646/zootaxa.3948.3.7.

1025 Whitenack LB, Gottfried MD. 2010. A morphometric approach for addressing tooth-based
1026 species delimitation in fossil mako sharks, *Isurus* (Elasmobranchii: Lamniformes). *Journal*
1027 *of Vertebrate Paleontology* 30:17–25 DOI: 10.1080/02724630903409055.

1028 Whitley GP. 1929. Studies in ichthyology. *Records of the Australian Museum* 17:101–143.

1029 Wilmers J, Waldron M, Bargmann S. 2021. Hierarchical microstructure of tooth enameloid in
1030 two Lamniform shark species, *Carcharias taurus* and *Isurus oxyrinchus*. *Nanomaterials*
1031 11:969 DOI: 10.3390/nano11040969.

1032 Xue W-J. 2004. *Chiayi area fossil map*. Chiayi: Chiayi City Cultural Bureau.

1033 Yabumoto Y, Uyeno T. 1994. Late Mesozoic and Cenozoic fish faunas of Japan. *Island Arc*
1034 3:255–269 DOI: 10.1111/j.1440-1738.1994.tb00115.x.

1035 Yu H-S, Chou Y-W. 2001. Characteristics and development of the flexural forebulge and basal
1036 unconformity of Western Taiwan Foreland Basin. *Tectonophysics* 333:277–291.

1037 Yudha DS, Ramadhani R, Suryianto RA, Novian MI. 2018. The diversity of sharks fossils in
1038 Plio-Pleistocene of Java, Indonesia. *AIP Conference Proceedings* 2002(1):020013
1039 DOI: 10.1063/1.5050109.

1040

1041 **Supplemental file**

1042 Supplemental Figure S1. Aerial photographs of the Niubu locality showing the closest
1043 sampling site to the weir (red square, Site 1 in Fig. 2B). A, general view; B, C, closer views
1044 of the sampling site. Note the sandstones in the river bed transported from the upstream
1045 older strata.

1046 Supplemental Table S1. List of taxa and their abundance extracted from the Pleistocene
1047 elasmobranch assemblages from the West Pacific. Only teeth are included, i.e., spines, vertebrae
1048 and other remains are not **considered**. Nomenclatures remain as those reported in the literature.

1049 Supplemental Table S2. Measurement, tooth position, and estimated fish total length of 44
1050 better-preserved specimens of *Carcharodon carcharias* specimens **form** the early
1051 Pleistocene of Liuchungchi Formation of Niubu, southern Taiwan. * = estimated crown
1052 height values for specimens with slightly worn apex.

1053

1054 **Figure captions**

1055 Figure 1. Summary of the sampling sites. A, overview of geological map of Taiwan (modified
1056 after Chen, 2016). B, geological map of Nuibu area, Chiayi (map extracted from National
1057 Geological Data Warehouse, Central Geological Survey, MOEA). Yellow stars = sampling sites
1058 (see Fig. 2B for details). C, stratigraphic correlation of the Western Foothills (modified after
1059 Chen, 2016). **The examined** Liuchungchi Formation is indicated in red.

1060

1061 Figure 2. A, stratigraphic column (modified after Huang, 2010). B, details of the sampling sites.
1062 GPS coordinates: Site 1 = 23°26'23.4"N, 120°35'35.5"E; Site 2 = 23°26'22.6"N, 120°35'32.7"E;
1063 Site 3 = 23°26'23.5"N, 120°35'29.8"E.

1064

1065 Figure 3. Teeth of *Carcharias taurus* from the early Pleistocene **of** Liuchungchi Formation of
1066 Niubu, southern Taiwan. A, B, ASIZF0100320; C, D, E, CMM F0204. A, C = lingual views; B,
1067 D = labial views; E = lateral view. Scale bar = 1 cm.

1068

1069 Figure 4. Teeth of *Carcharodon carcharias* from the early Pleistocene **of** Liuchungchi Formation
1070 of Niubu, southern Taiwan. A, B, ASIZF0100344; C, D, ASIZF0100337; E, F, ASIZF0100338;
1071 G, H, ASIZF0100336; I, J, ASIZF0100335; K, L, ASIZF0100339; M, N, ASIZF0100340; O, P,
1072 ASIZF0100324; Q, R, ASIZF0100328; S, T, ASIZF0100325; U, V, ASIZF0100326; W, X,
1073 ASIZF0100323. A, C, E, G, I, K, M, O, Q, S, U, W = lingual views; B, D, F, H, J, L, N, P, R, T,
1074 V, X = labial views. Scale bar = 1 cm.

1075

1076 Figure 5. Teeth of *Isurus oxyrinchus* from the early Pleistocene of Liuchungchi Formation of
1077 Niubu, southern Taiwan. A, B, C, ASIZF0100317; D, E, F, ASIZF0100318; G, H,
1078 ASIZF0100321; I, J, CMM F0242. A, D, G, I = lingual views; B, E, H, J = labial views; C, F =
1079 lateral views. Scale bar = 1 cm.

1080

1081 Figure 6. Teeth of †*Hemipristis serra* from the early Pleistocene of Liuchungchi Formation of
1082 Niubu, southern Taiwan. A, B, CMM F0232; C, D, ASIZF0100460; E, F, ASIZF0100461; G, H,
1083 ASIZF0100462. A, C, E, G = lingual views; B, D, F, H = labial views. Scale bars = 1 cm.

1084

1085 Figure 7. Teeth of *Carcharhinus altimus* from the early Pleistocene of Liuchungchi Formation of
1086 Niubu, southern Taiwan. A, B, ASIZF0100357; C, D, ASIZF0100359; E, F, CMM F0363; G, H,
1087 CMM F0293; I, J, CMM F0322; K, L, ASIZF 0100365. A, C, E, G, I, K = lingual views; B, D,
1088 F, H, J, L = labial views. Scale bar = 1 cm.

1089

1090 Figure 8. Teeth of *Carcharhinus amboinensis* from the early Pleistocene of Liuchungchi
1091 Formation of Niubu, southern Taiwan. A, B, CMM F0209; C, D, ASIZF0100368; E, F,
1092 ASIZF0100366; G, H, ASIZF0100369. A, C, E, G = lingual views; B, D, F, H = labial views.
1093 Scale bar = 1 cm.

1094

1095 Figure 9. Teeth of *Carcharhinus leucas* from the early Pleistocene of Liuchungchi Formation of
1096 Niubu, southern Taiwan. A, B, ASIZF0100398; C, D, ASIZF0100397; E, F, ASIZF0100394; G,
1097 H, ASIZF0100411; I, J, ASIZF0100396; K, L, ASIZF 0100395; M, N, ASIZF0100400; O, P,
1098 ASIZF0100402; Q, R, ASIZF0100390. A, C, E, G, I, K, M, O, Q = lingual views; B, D, F, H, J,
1099 L, N, P, R = labial views. Scale bar = 1 cm.

1100

1101 Figure 10. Teeth of *Carcharhinus limbatus* from the early Pleistocene of Liuchungchi Formation
1102 of Niubu, southern Taiwan. A, B, ASIZF0100470; C, D, ASIZF0100476; E, F, ASIZF0100469;
1103 G, H, ASIZF0100468; I, J, CMM F0236; K, L, CMM F0111; M, N, CMM F0237; O, P, CMM
1104 F0238. A, C, E, G, I, K, M, O = lingual views; B, D, F, H, J, L, N, P = labial views. Scale bar = 1
1105 cm.

1106

1107 Figure 11. Teeth of *Carcharhinus longimanus* from the early Pleistocene of Liuchungchi
1108 Formation of Niubu, southern Taiwan. A, B, ASIZF 0100371; C, D, ASIZF0100376; E, F,
1109 ASIZF0100370; G, H, ASIZF0100377; I, J, ASIZF0100375; K, L, ASIZF0100378; M, N,
1110 ASIZF0100374; O, P, ASIZF0100373; Q, R, ASIZF0100392; S, T, ASIZF0100391. A, C, E, G,
1111 I, K, M, O, Q, S = lingual views; B, D, F, H, J, L, N, P, R, T = labial views. Scale bar = 1 cm.

1112

1113 Figure 12. Teeth of *Carcharhinus obscurus* from the early Pleistocene of Liuchungchi Formation
1114 of Niubu, southern Taiwan. A, B, ASIZF0100372; C, D, ASIZF0100384; E, F, ASIZF0100385;

1115 G, H, ASIZF0100386; I, J, ASIZF0100388; K, L, ASIZF0100387; M, N, ASIZF0100383. A, C,
1116 E, G, I, K, M = lingual views; B, D, F, H, J, L, N = labial views. Scale bar = 1 cm.

1117

1118 Figure 13. Teeth of *Carcharhinus plumbeus* from the early Pleistocene of Liuchungchi
1119 Formation of Niubu, southern Taiwan. A, B, ASIZF0100412; C, D, ASIZF0100406; E, F,
1120 ASIZF0100405; G, H, ASIZF0100410; I, J, ASIZF0100409; K, L, ASIZF0100408; M, N,
1121 ASIZF0100407. A, C, E, G, I, K, M = lingual views; B, D, F, H, J, L, N = labial views. Scale bar
1122 = 1 cm.

1123

1124 Figure 14. Teeth of *Carcharhinus sorrah* from the early Pleistocene of Liuchungchi Formation
1125 of Niubu, southern Taiwan. A, B, CMM F0129; C, D, CMM F0119; E, F, ASIZF0100418; G, H,
1126 CMM F0126; I, J, CMM F0135; K, L, CMM F0122; M, N, CMM F0140. A, C, E, G, I, K, M =
1127 lingual views; B, D, F, H, J, L, N = labial views. Scale bar = 1 cm.

1128

1129 Figure 15. Teeth of *Carcharhinus tjutjot* from the early Pleistocene of Liuchungchi Formation of
1130 Niubu, southern Taiwan. A, B, ASIZF0100415; C, D, ASIZF0100414; E, F, CMM F0116; G, H,
1131 ASIZF0100413; I, J, ASIZF0100417; K, L, ASIZF0100416; M, N, CMM F0323; O, P, CMM
1132 F0324. A, C, E, G, I, K, M, O = lingual views; B, D, F, H, J, L, N, P = labial views. Scale bar = 1
1133 cm.

1134

1135 Figure 16. Teeth of *Rhizoprionodon acutus* from the early Pleistocene of Liuchungchi Formation
1136 of Niubu, southern Taiwan. A, B, ASIZF0100463; C, D, CMM F0120; E, F, CMM F0121; G, H,
1137 CMM F0131; I, J, ASIZF0100464. A, C, E, G, I = lingual views; B, D, F, H, J = labial views.
1138 Scale bar = 1 cm.

1139

1140 Figure 17. Teeth of *Galeocerdo cuvier* and *Sphyraena lewini* from the early Pleistocene of
1141 Liuchungchi Formation of Niubu, southern Taiwan. A–H, *Galeocerdo cuvier*; A, B, CMM
1142 F0245; C, D, E, CMM F0215; F, G, H, ASIZF0100459. I–L, *Sphyraena lewini*; I, J, CMM F0235;
1143 K, L, CMM F0312. A, C, F, I, K = lingual views; B, D, G, J, L = labial views; E, H = details of
1144 secondary serrations. Scale bars = 1 cm.

1145

1146 Figure 18. Teeth of Dasyatidae indet. from the early Pleistocene of Liuchungchi Formation of
1147 Niubu, southern Taiwan. A, B, C, D, ASIZF0100590; E, F, G, H, ASIZF0100591. A, E = labial
1148 views; B, F = basal views; C, G = occlusal views; D, H = lateral views. Scale bar = 5 mm.

1149

1150 Figure 19. Teeth of *Aetobatus* sp. from the early Pleistocene of Liuchungchi Formation of Niubu,
1151 southern Taiwan. A, B, CMM F2854; C, D, CMM F2850; E, F, CMM F0408; G, H,
1152 ASIZF0100549. A, C, E, G = occlusal views; B, D, F, H = basal views. Scale bar = 1 cm.

1153

1154 Figure 20. Teeth of *Myliobatis* sp. from the early Pleistocene of Liuchungchi Formation of
1155 Niubu, southern Taiwan. A, B, C, D, ASIZF0100582; E, F, G, H, ASIZF0100587; I, J, K, L,
1156 ASIZF0100586; M, N, CMM F0395; O, P, CMM F2855; Q, R, CMM F0393; S, T, CMM

1157 F0398. A, E, I, M, O, Q, S = occlusal views; B, F, J, N, P, R, T = basal views; C, G, K = lingual
1158 views; D, H, L = labial views. Scale bars = 1 cm.

1159

1160

1161 **Table captions**

1162 Table 1. Elasmobranchs from the early Pleistocene Liuchungchi Formation of Niubu, southern
1163 Taiwan.

1164 Table 2. Various diversity indices from the Pleistocene West Pacific elasmobranch assemblages
1165 showing high diversity of the present material. See Supplemental Table S1 for details of the data.

Figure 1

Summary of the sampling sites.

A, overview of geological map of Taiwan (modified after Chen, 2016). B, geological map of Nuibu area, Chiayi (map extracted from National Geological Data Warehouse, Central Geological Survey, MOEA). Yellow stars = sampling sites (see Fig. 2B for details). C, stratigraphic correlation of the Western Foothills (modified after Chen, 2016). The examined Liuchungchi Formation is indicated in yellow.

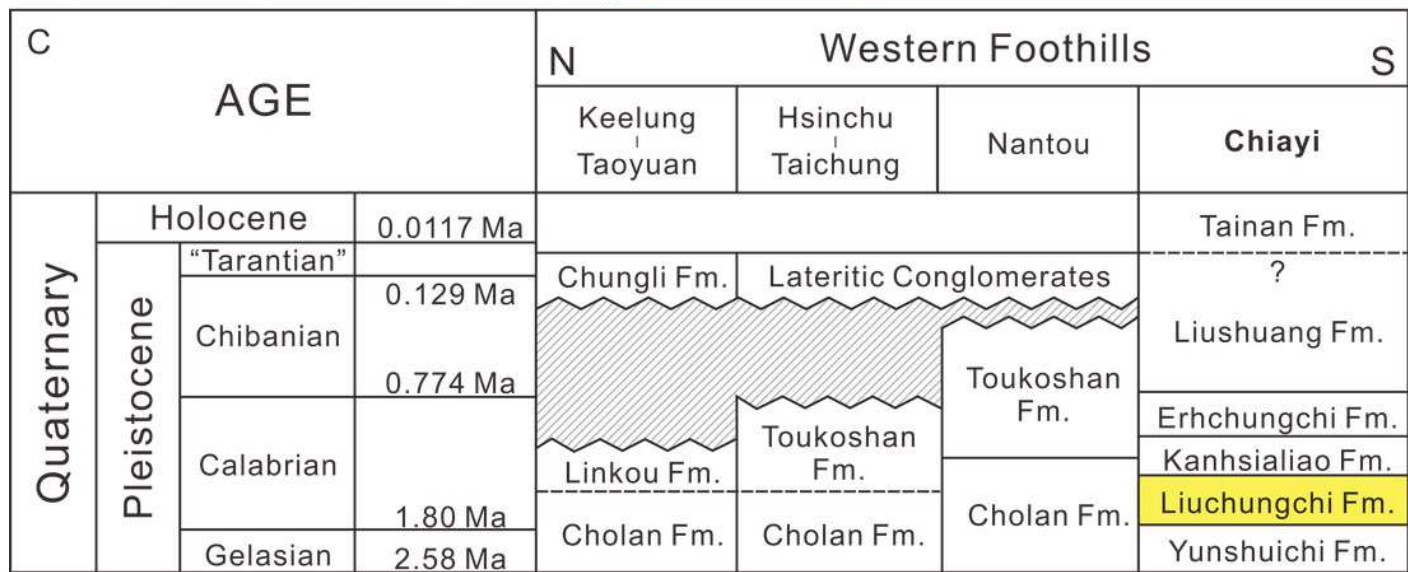
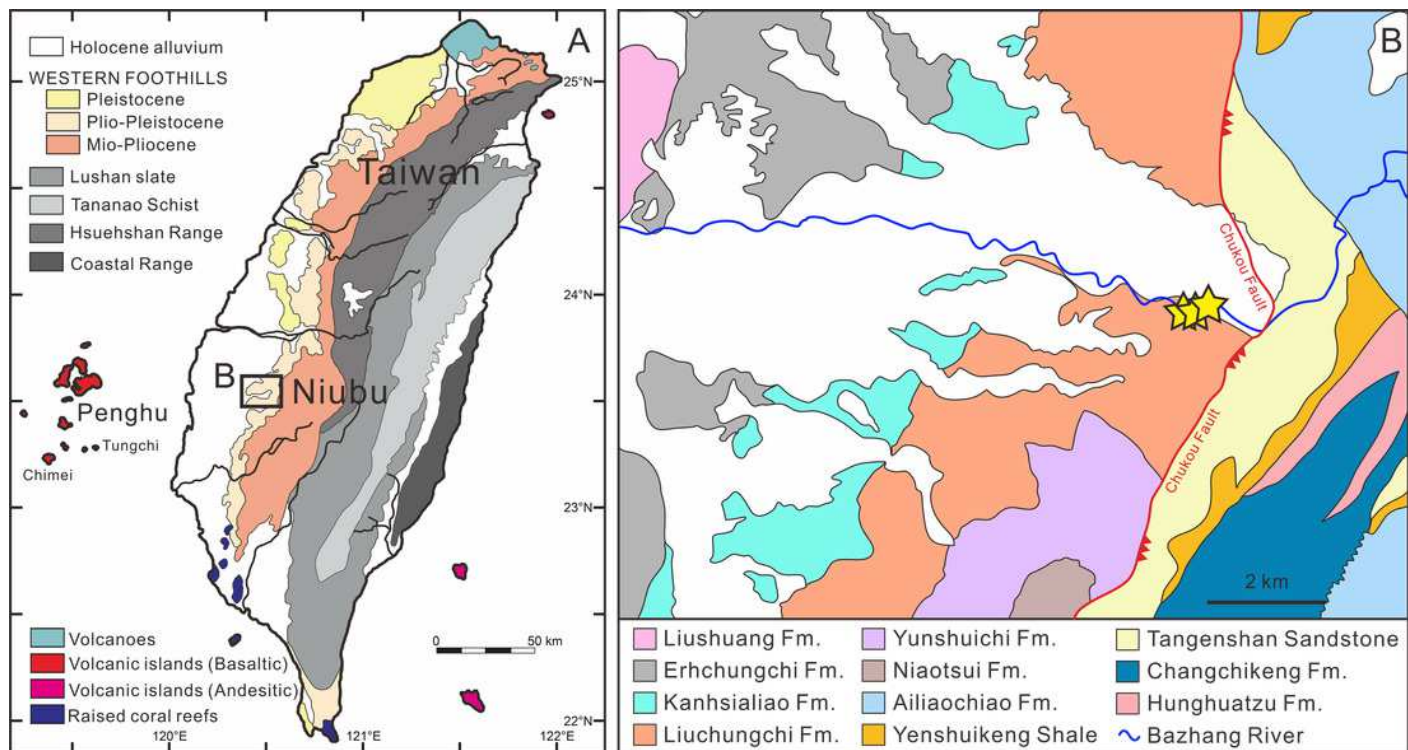


Figure 2

A, stratigraphic column (modified after Huang, 2010). B, details of the sampling sites.

GPS coordinates: Site 1 = $23^{\circ}26'23.4''\text{N}$, $120^{\circ}35'35.5''\text{E}$; Site 2 = $23^{\circ}26'22.6''\text{N}$,

$120^{\circ}35'32.7''\text{E}$; Site 3 = $23^{\circ}26'23.5''\text{N}$, $120^{\circ}35'29.8''\text{E}$.

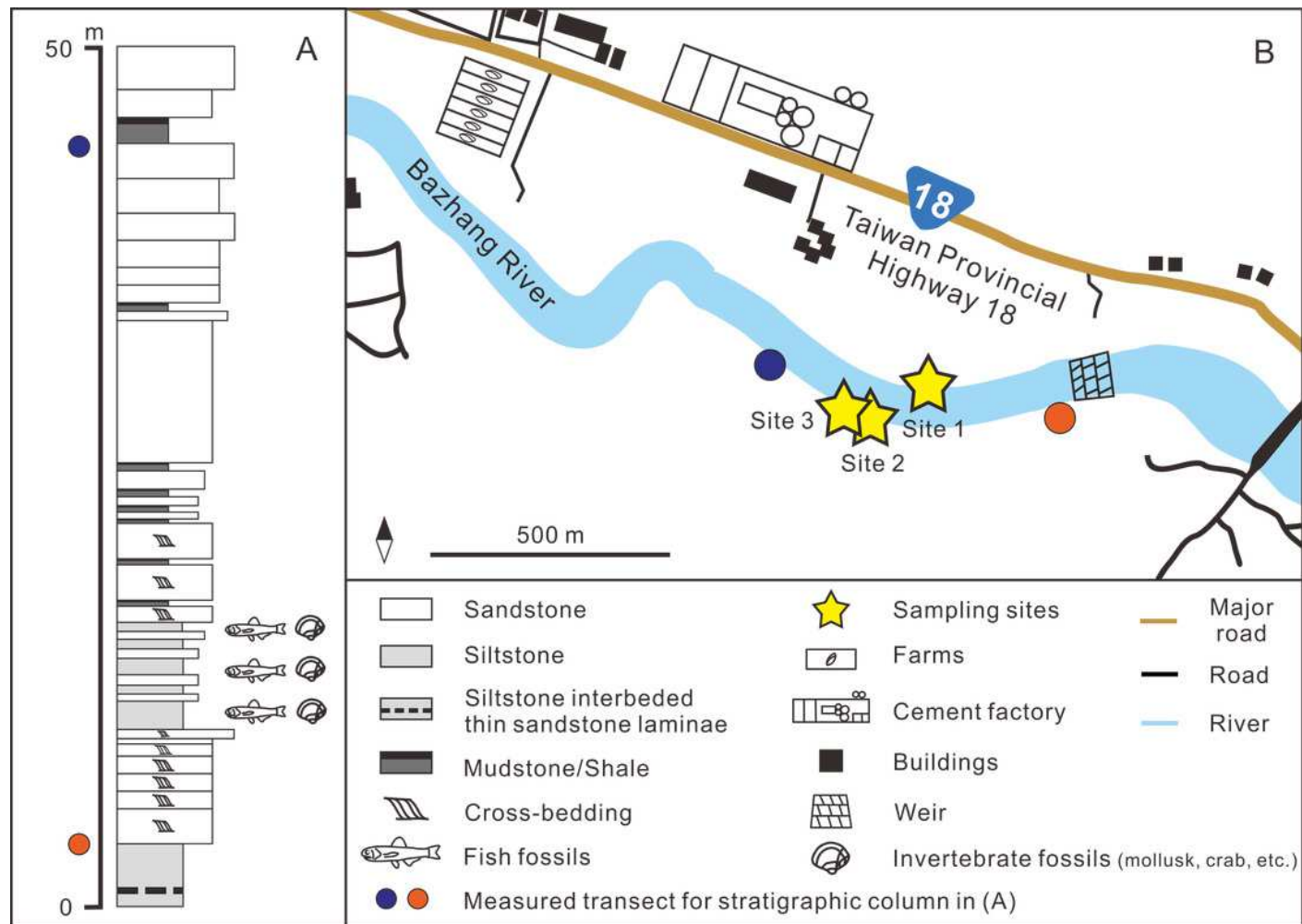


Figure 3

Teeth of *Carcharias taurus* from the early Pleistocene of Liuchungchi Formation of Niubu, southern Taiwan.

A, B, ASIZF0100320; C, D, E, CMM F0204. A, C = lingual views; B, D = labial views; E = lateral view. Scale bar = 1 cm.

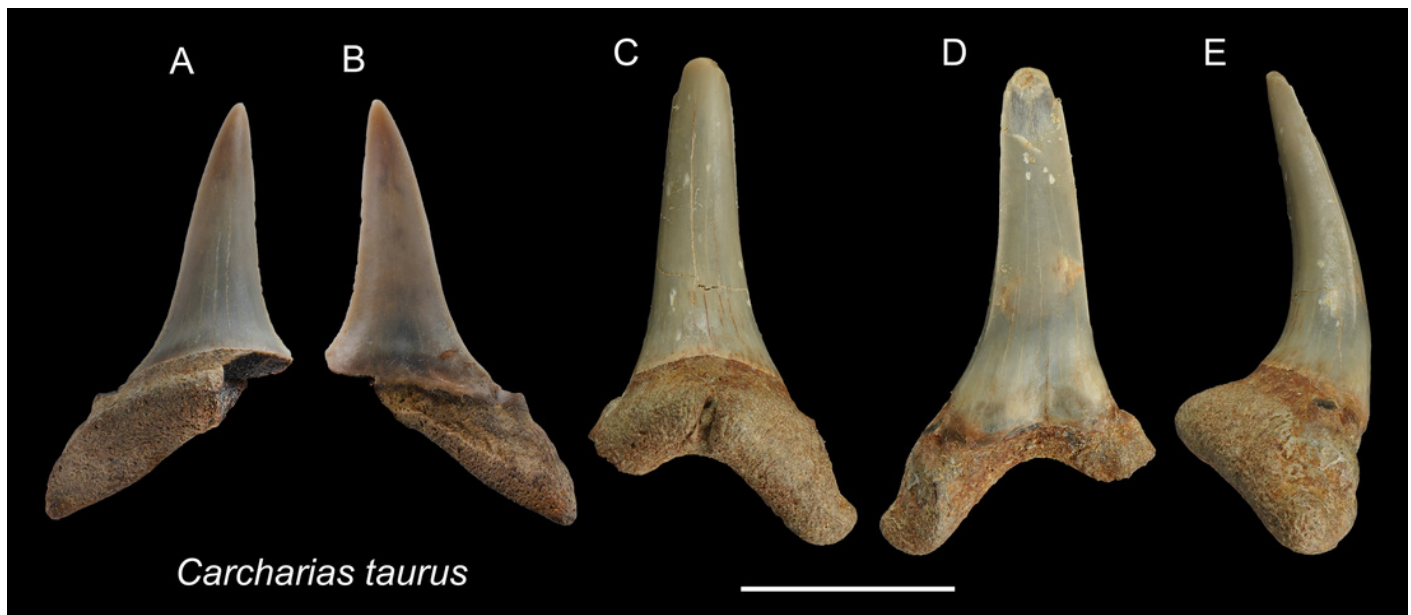


Figure 4

Teeth of *Carcharodon carcharias* from the early Pleistocene of Liuchungchi Formation of Niubu, southern Taiwan.

A, B, ASIZF0100344; C, D, ASIZF0100337; E, F, ASIZF0100338; G, H, ASIZF0100336; I, J, ASIZF0100335; K, L, ASIZF0100339; M, N, ASIZF0100340; O, P, ASIZF0100324; Q, R, ASIZF0100328; S, T, ASIZF0100325; U, V, ASIZF0100326; W, X, ASIZF0100323. A, C, E, G, I, K, M, O, Q, S, U, W = lingual views; B, D, F, H, J, L, N, P, R, T, V, X = labial views. Scale bar = 1 cm.

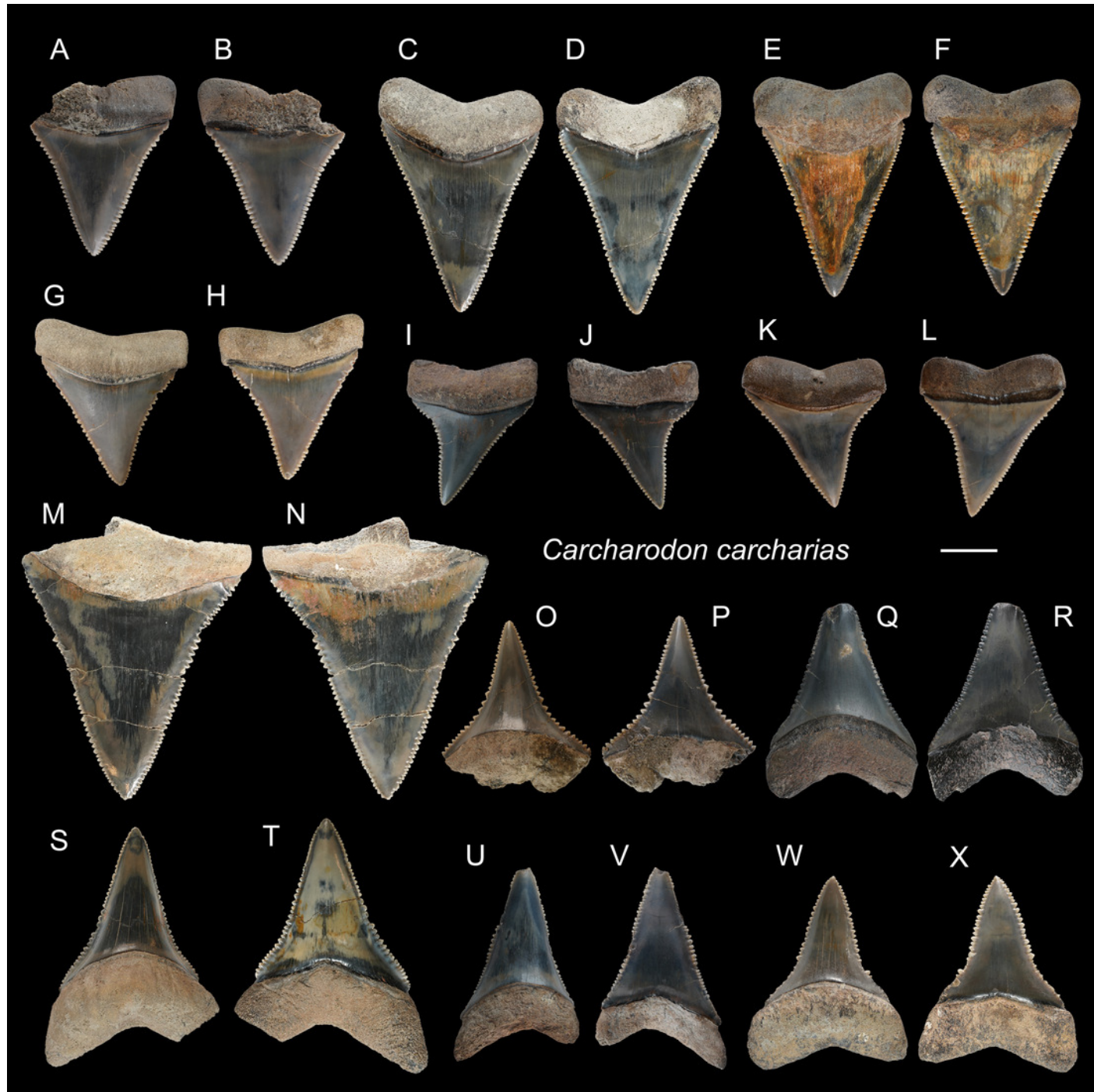


Figure 5

Teeth of *Isurus oxyrinchus* from the early Pleistocene of Liuchungchi Formation of Niubu, southern Taiwan.

A, B, C, ASIZF0100317; D, E, F, ASIZF0100318; G, H, ASIZF0100321; I, J, CMM F0242. A, D, G, I = lingual views; B, E, H, J = labial views; C, F = lateral views. Scale bar = 1 cm.

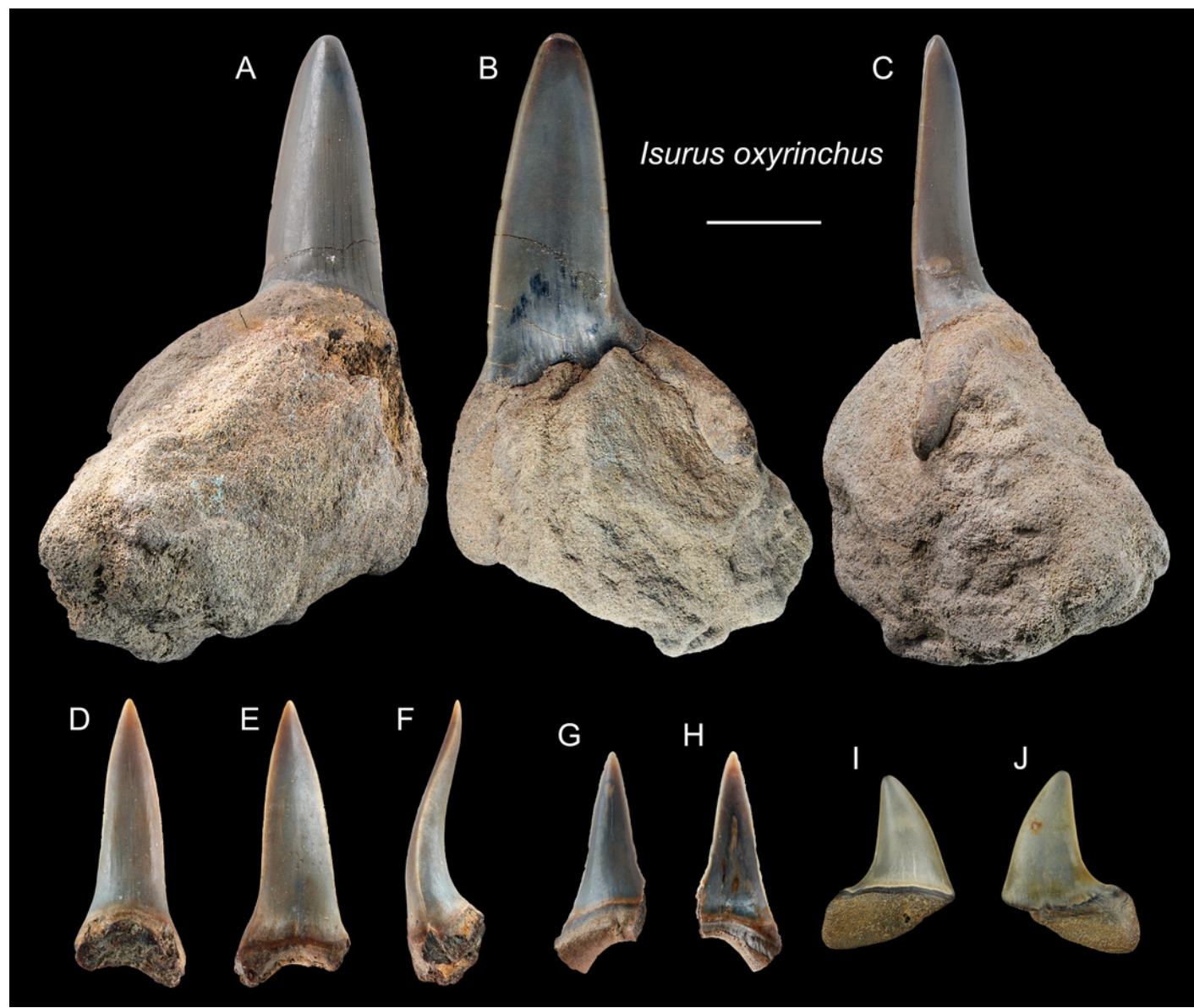


Figure 6

Teeth of †*Hemipristis serra* from the early Pleistocene of Liuchungchi Formation of Niubu, southern Taiwan.

A, B, CMM F0232; C, D, ASIZF0100460; E, F, ASIZF0100461; G, H, ASIZF0100462. A, C, E, G = lingual views; B, D, F, H = labial views. Scale bars = 1 cm.

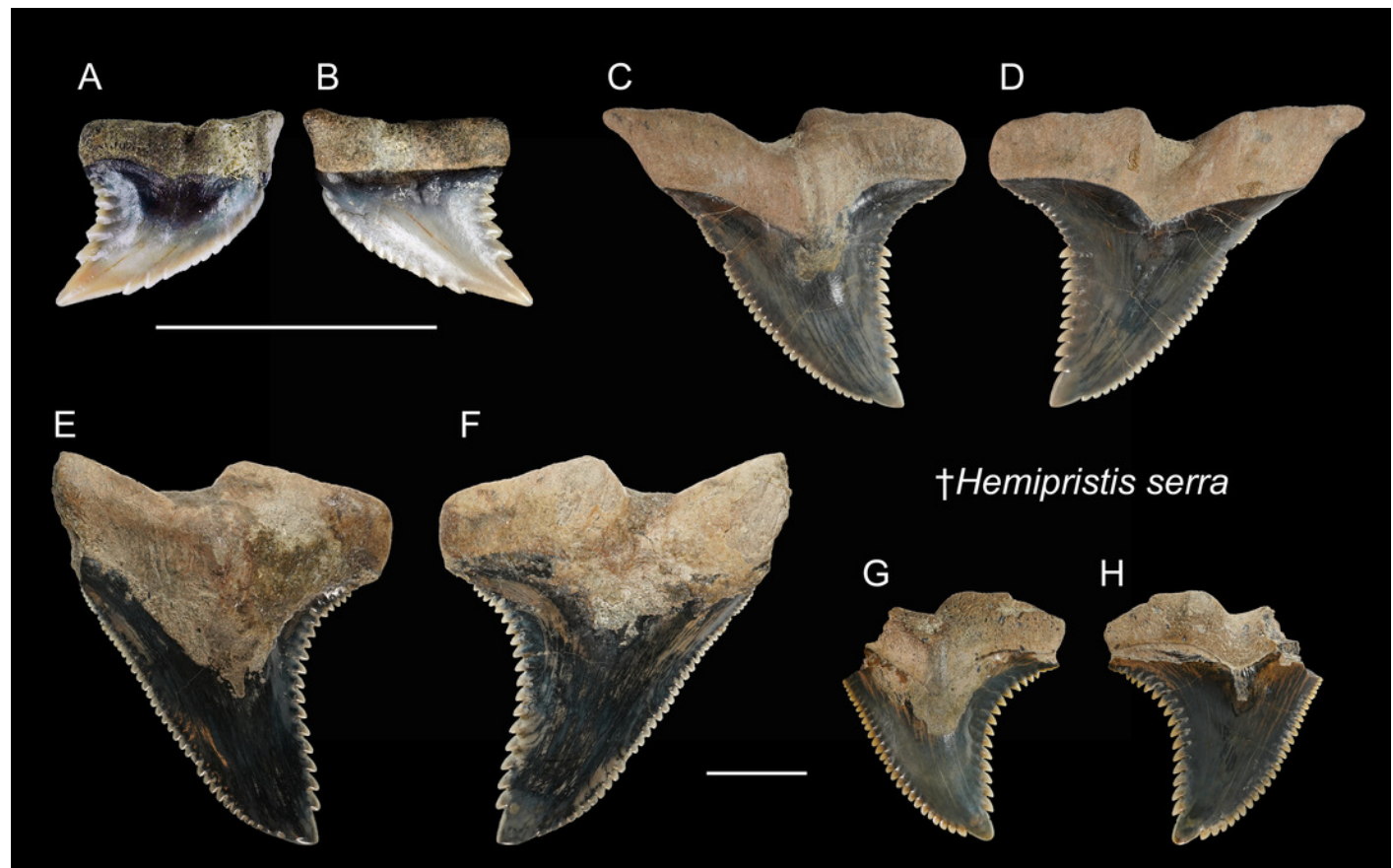


Figure 7

Teeth of *Carcharhinus altimus* from the early Pleistocene of Liuchungchi Formation of Niubu, southern Taiwan.

A, B, ASIZF0100357; C, D, ASIZF0100359; E, F, CMM F0363; G, H, CMM F0293; I, J, CMM F0322; K, L, ASIZF 0100365. A, C, E, G, I, K = lingual views; B, D, F, H, J, L = labial views. Scale bar = 1 cm.

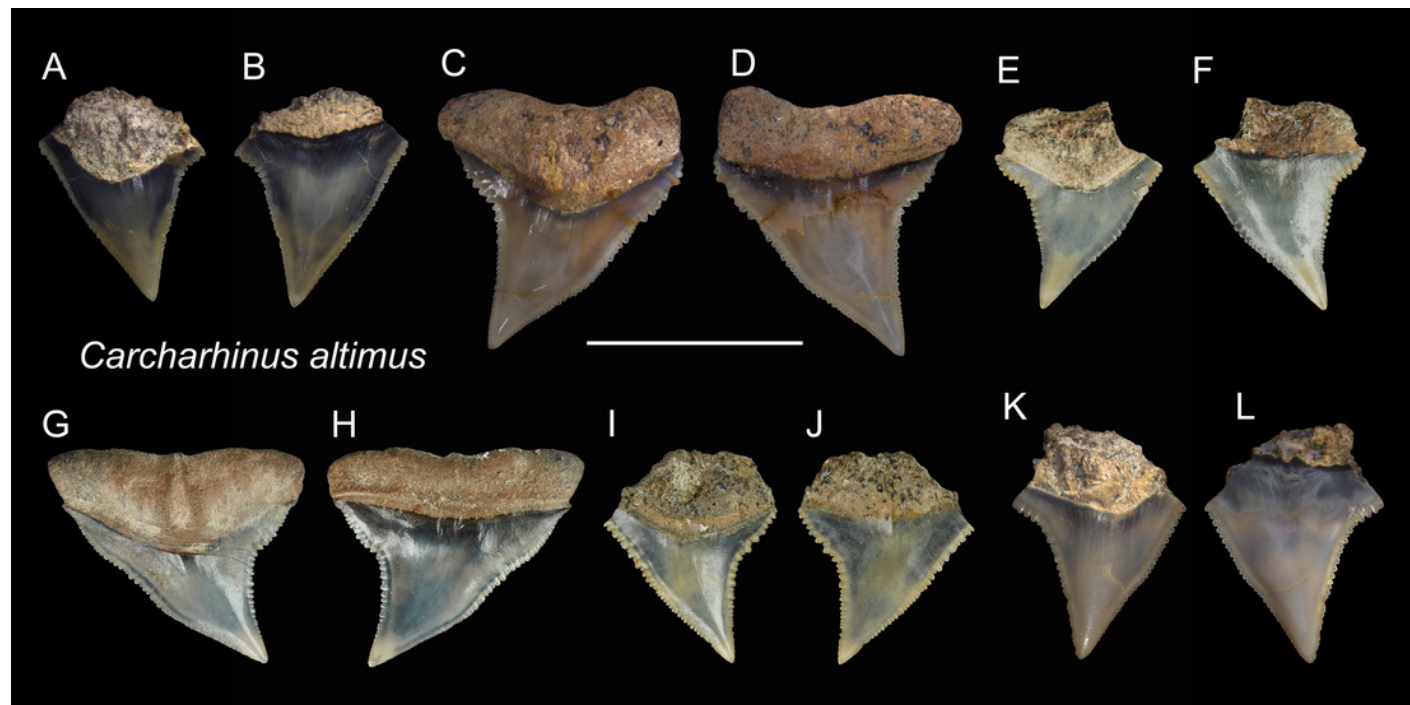


Figure 8

Teeth of *Carcharhinus amboinensis* from the early Pleistocene of Liuchungchi Formation of Niubu, southern Taiwan.

A, B, CMM F0209; C, D, ASIZF0100368; E, F, ASIZF0100366; G, H, ASIZF0100369. A, C, E, G = lingual views; B, D, F, H = labial views. Scale bar = 1 cm.

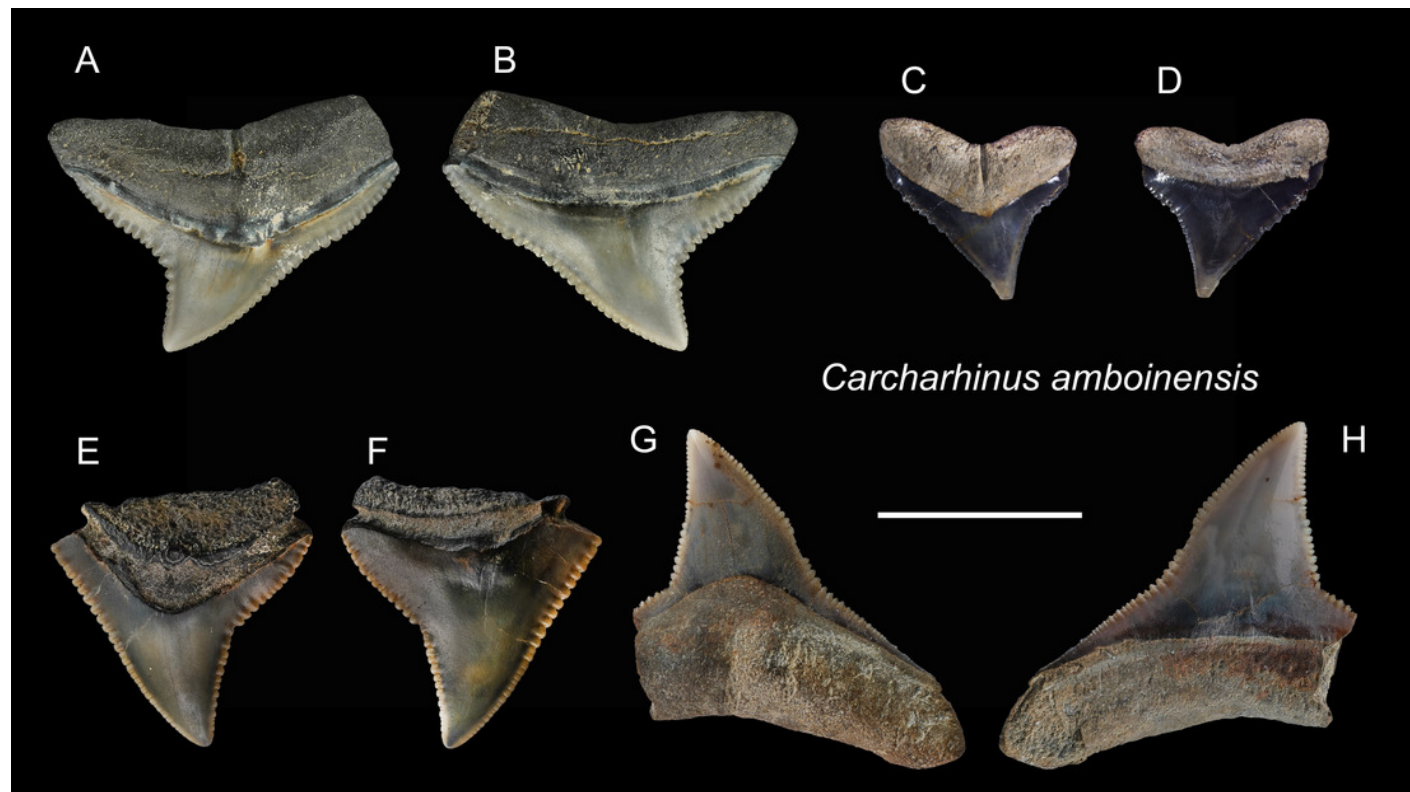


Figure 9

Teeth of *Carcharhinus leucas* from the early Pleistocene of Liuchungchi Formation of Niubu, southern Taiwan.

A, B, ASIZF0100398; C, D, ASIZF0100397; E, F, ASIZF0100394; G, H, ASIZF0100411; I, J, ASIZF0100396; K, L, ASIZF 0100395; M, N, ASIZF0100400; O, P, ASIZF0100402; Q, R, ASIZF0100390. A, C, E, G, I, K, M, O, Q = lingual views; B, D, F, H, J, L, N, P, R = labial views. Scale bar = 1 cm.

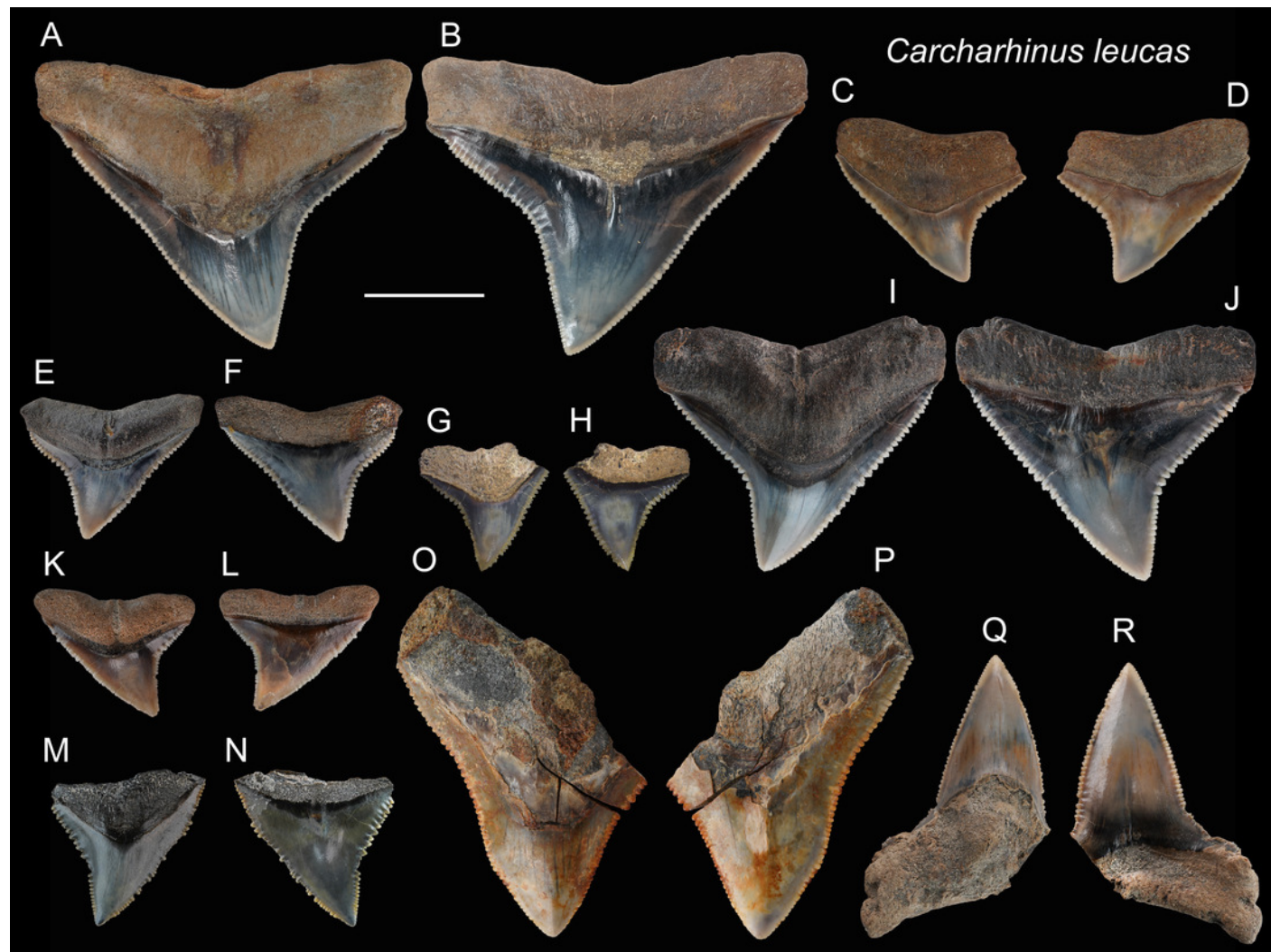


Figure 10

Teeth of *Carcharhinus limbatus* from the early Pleistocene of Liuchungchi Formation of Niubu, southern Taiwan.

A, B, ASIZF0100470; C, D, ASIZF0100476; E, F, ASIZF0100469; G, H, ASIZF0100468; I, J, CMM F0236; K, L, CMM F0111; M, N, CMM F0237; O, P, CMM F0238. A, C, E, G, I, K, M, O = lingual views; B, D, F, H, J, L, N, P = labial views. Scale bar = 1 cm.

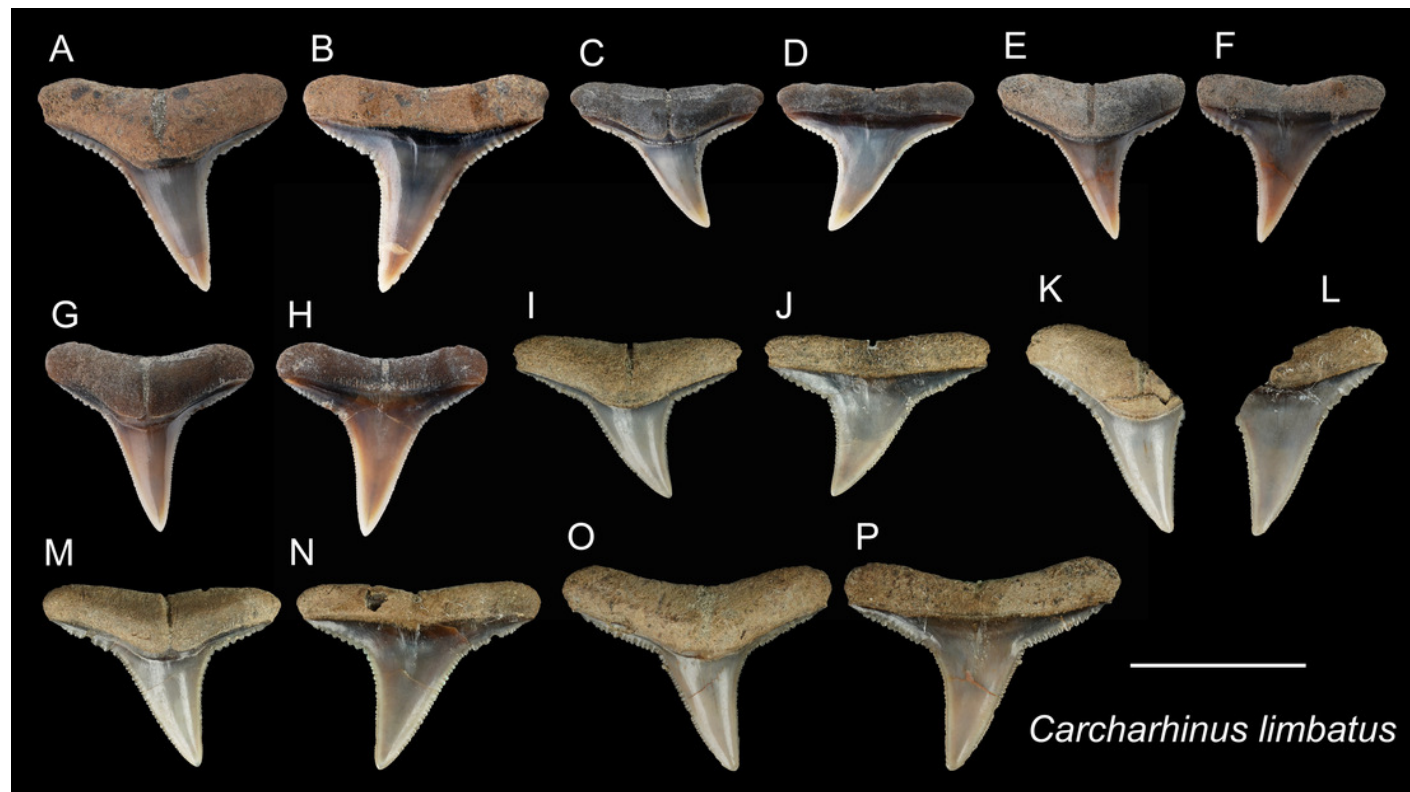


Figure 11

Teeth of *Carcharhinus longimanus* from the early Pleistocene of Liuchungchi Formation of Niubu, southern Taiwan.

A, B, ASIZF 0100371; C, D, ASIZF0100376; E, F, ASIZF0100370; G, H, ASIZF0100377; I, J, ASIZF0100375; K, L, ASIZF0100378; M, N, ASIZF0100374; O, P, ASIZF0100373; Q, R, ASIZF0100392; S, T, ASIZF0100391. A, C, E, G, I, K, M, O, Q, S = lingual views; B, D, F, H, J, L, N, P, R, T = labial views. Scale bar = 1 cm.

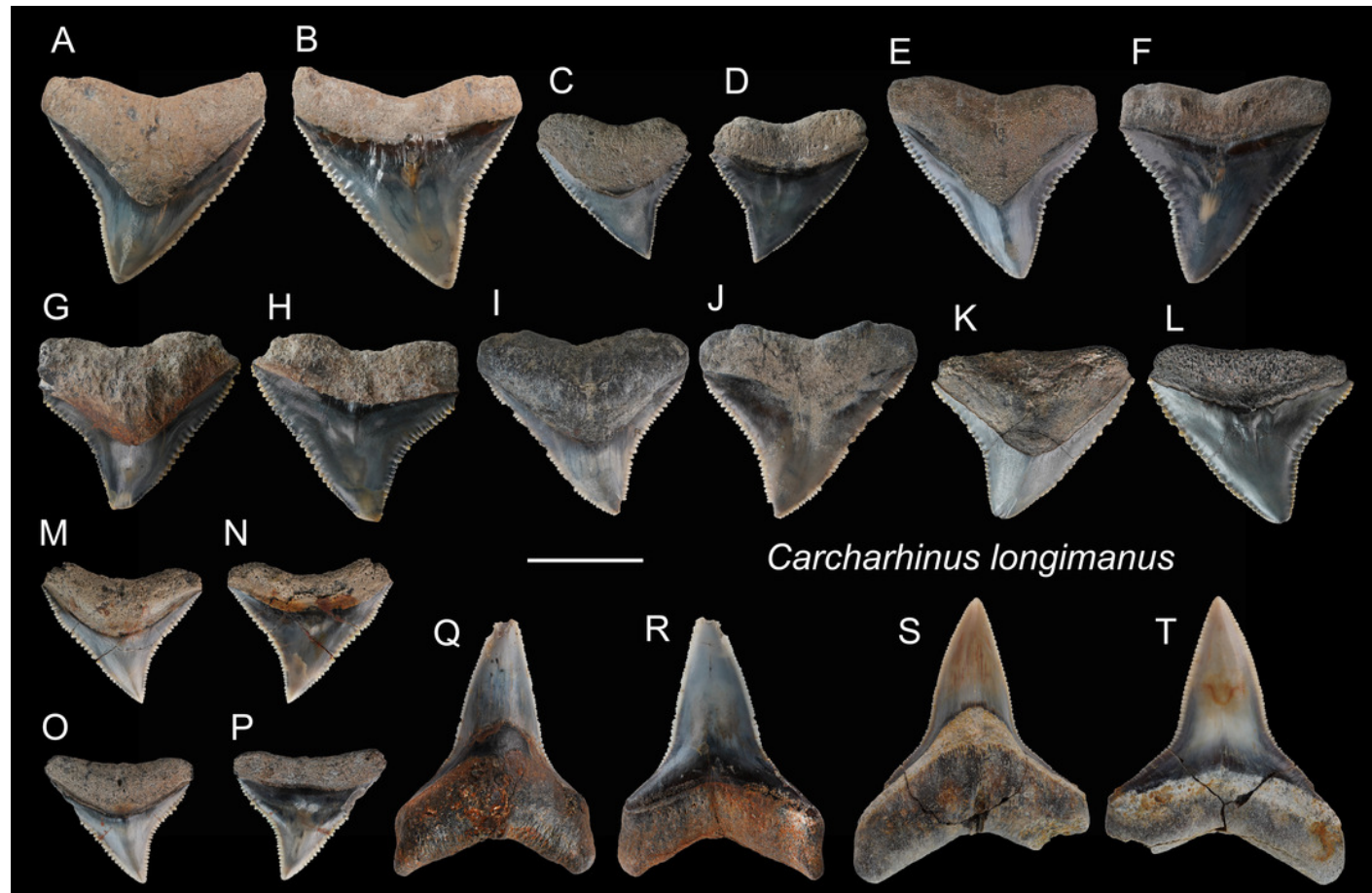


Figure 12

Teeth of *Carcharhinus obscurus* from the early Pleistocene of Liuchungchi Formation of Niubu, southern Taiwan.

A, B, ASIZF0100372; C, D, ASIZF0100384; E, F, ASIZF0100385; G, H, ASIZF0100386; I, J, ASIZF0100388; K, L, ASIZF0100387; M, N, ASIZF0100383. A, C, E, G, I, K, M = lingual views; B, D, F, H, J, L, N = labial views. Scale bar = 1 cm.

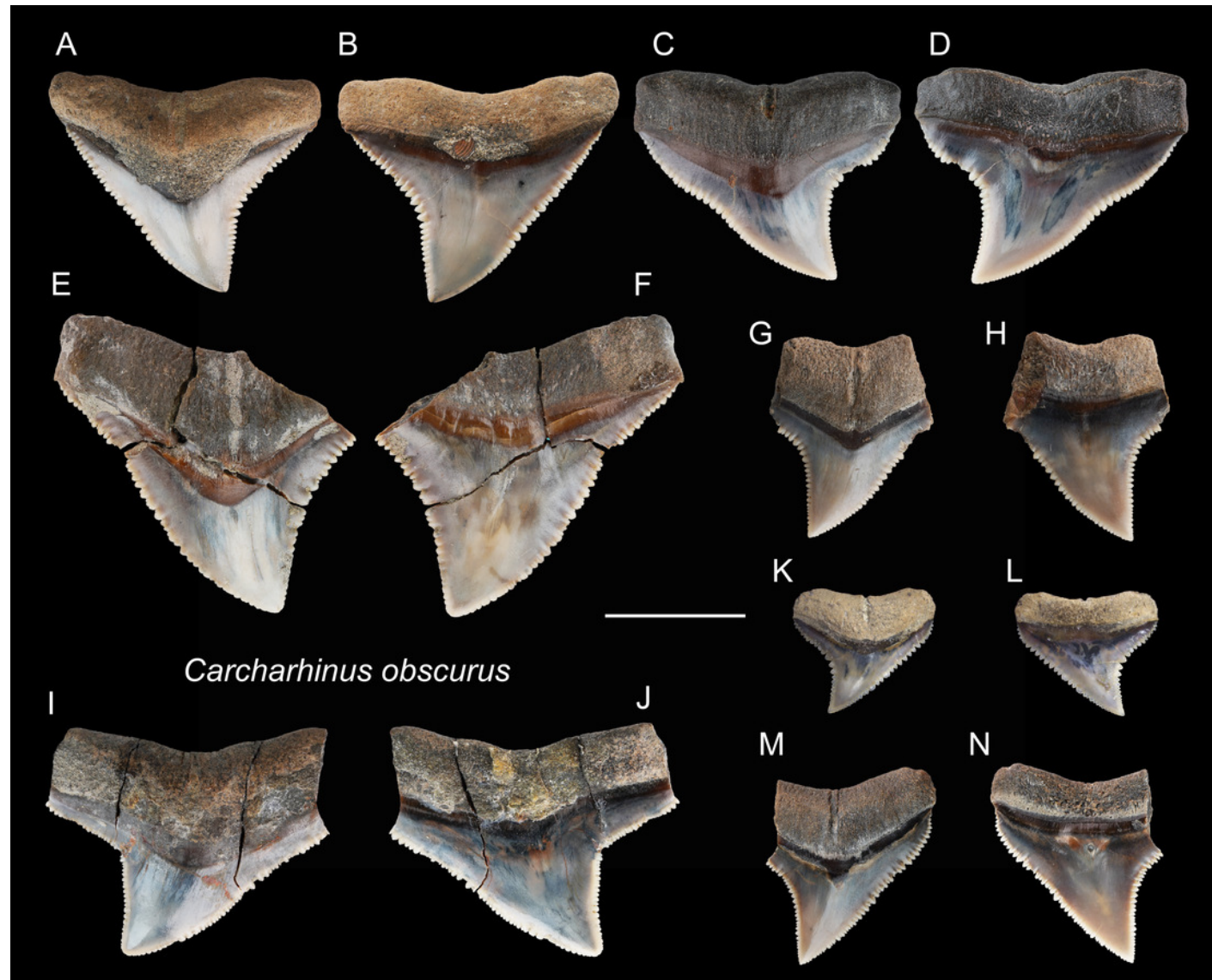


Figure 13

Teeth of *Carcharhinus plumbeus* from the early Pleistocene of Liuchungchi Formation of Niubu, southern Taiwan.

A, B, ASIZF0100412; C, D, ASIZF0100406; E, F, ASIZF0100405; G, H, ASIZF0100410; I, J, ASIZF0100409; K, L, ASIZF0100408; M, N, ASIZF0100407. A, C, E, G, I, K, M = lingual views; B, D, F, H, J, L, N = labial views. Scale bar = 1 cm.

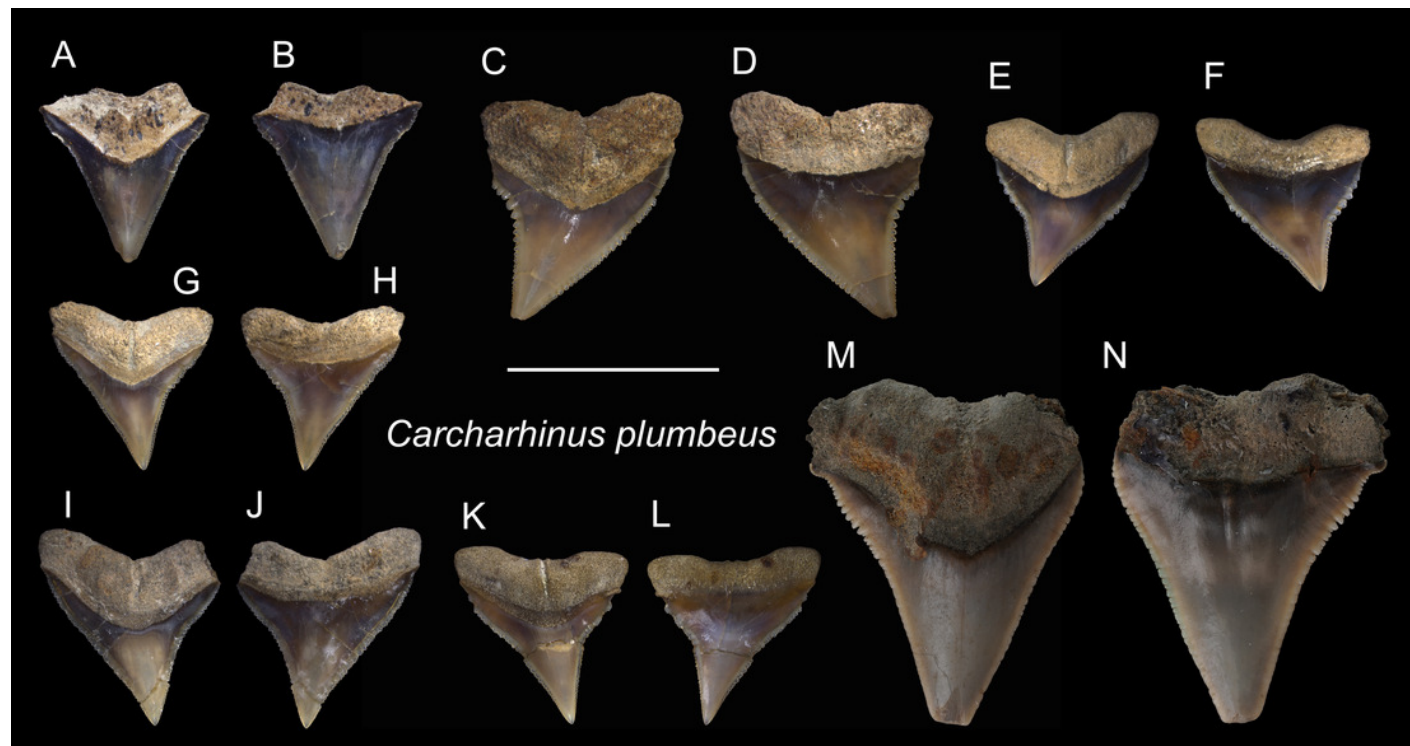


Figure 14

Teeth of *Carcharhinus sorrah* from the early Pleistocene of Liuchungchi Formation of Niubu, southern Taiwan.

A, B, CMM F0129; C, D, CMM F0119; E, F, ASIZF0100418; G, H, CMM F0126; I, J, CMM F0135; K, L, CMM F0122; M, N, CMM F0140. A, C, E, G, I, K, M = lingual views; B, D, F, H, J, L, N = labial views. Scale bar = 1 cm.

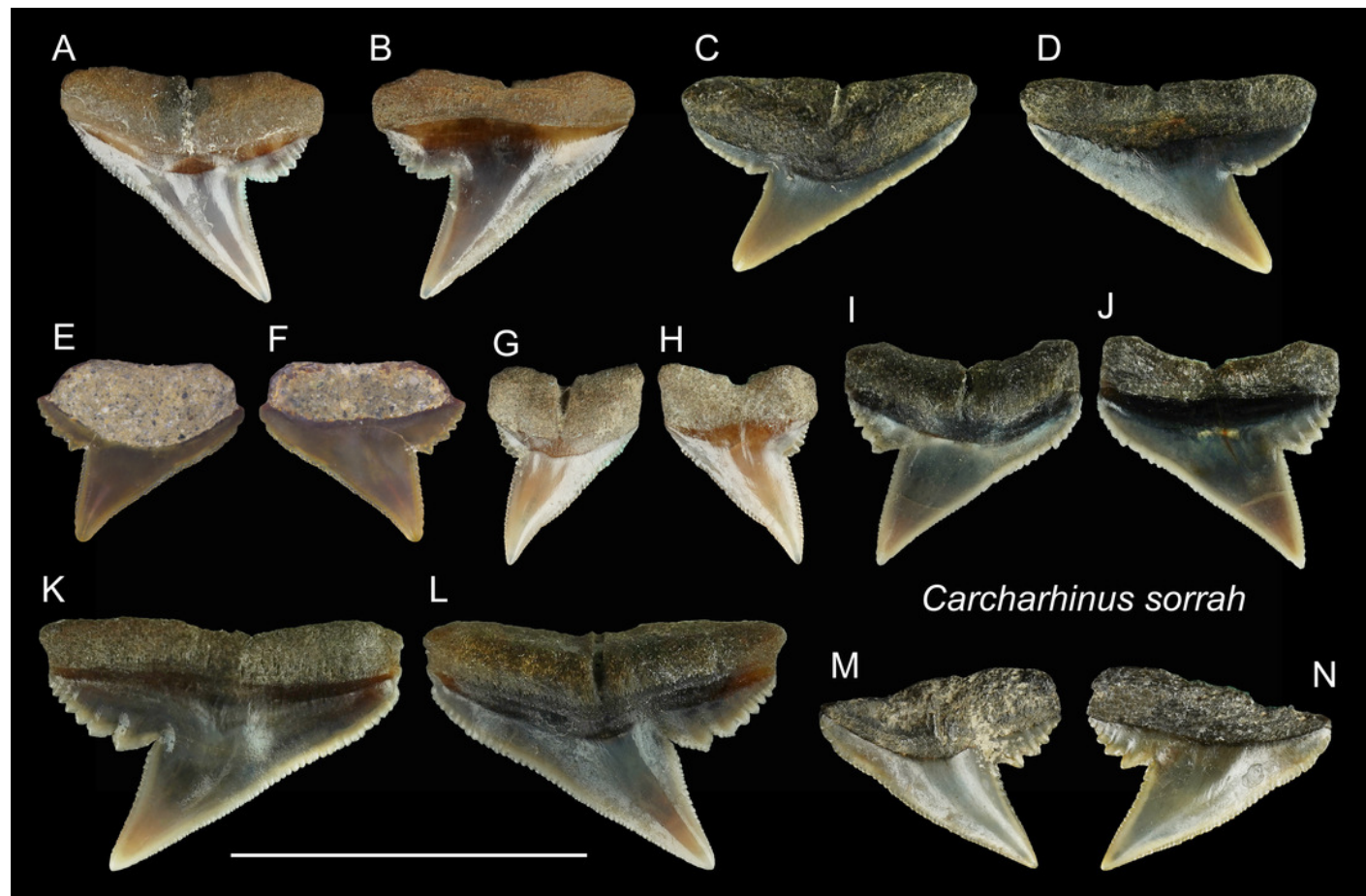


Figure 15

Teeth of *Carcharhinus tjutjot* from the early Pleistocene of Liuchungchi Formation of Niubu, southern Taiwan.

A, B, ASIZF0100415; C, D, ASIZF0100414; E, F, CMM F0116; G, H, ASIZF0100413; I, J, ASIZF0100417; K, L, ASIZF0100416; M, N, CMM F0323; O, P, CMM F0324. A, C, E, G, I, K, M, O = lingual views; B, D, F, H, J, L, N, P = labial views. Scale bar = 1 cm.

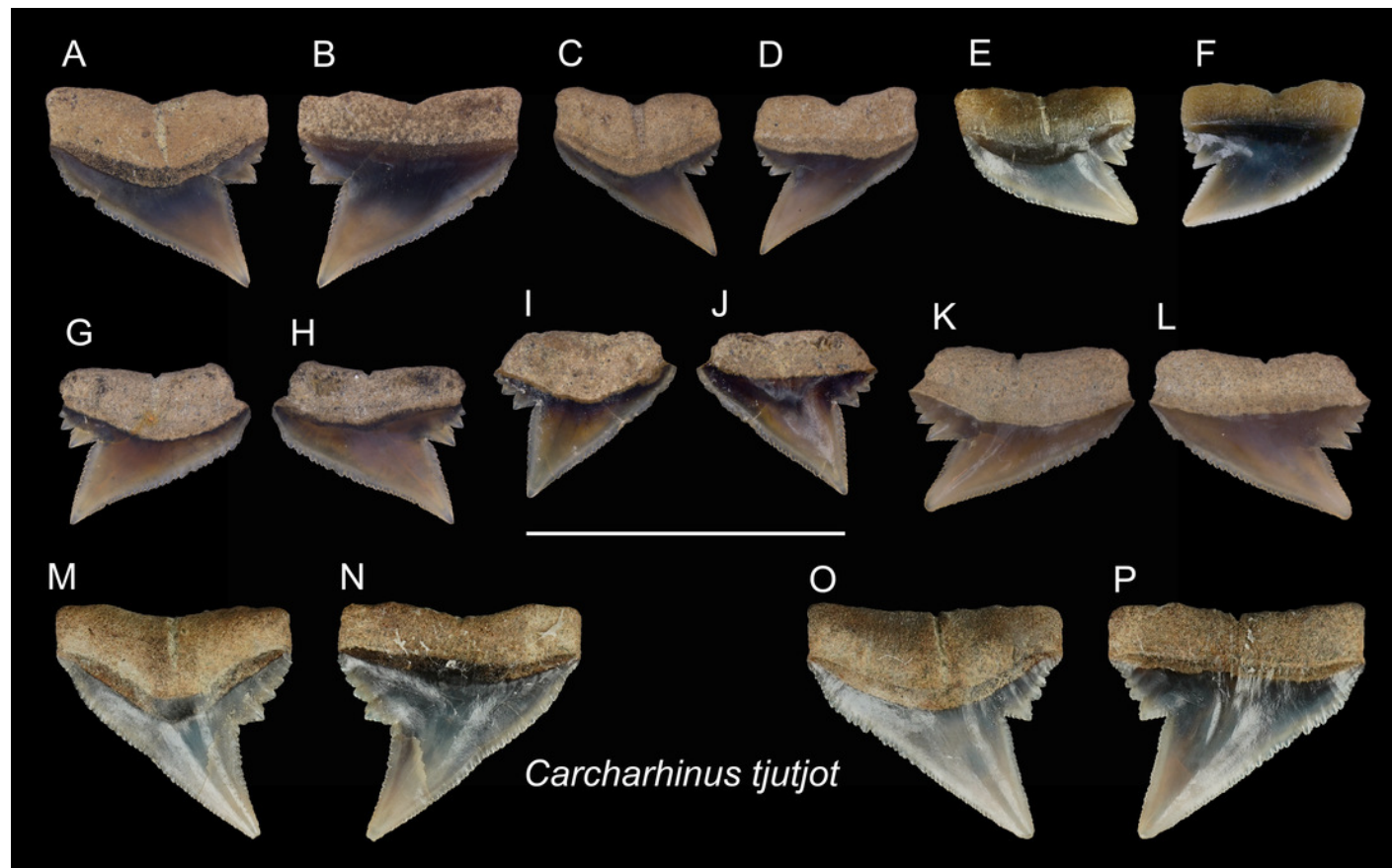


Figure 16

Teeth of *Rhizoprionodon acutus* from the early Pleistocene of Liuchungchi Formation of Niubu, southern Taiwan.

A, B, ASIZF0100463; C, D, CMM F0120; E, F, CMM F0121; G, H, CMM F0131; I, J, ASIZF0100464. A, C, E, G, I = lingual views; B, D, F, H, J = labial views. Scale bar = 1 cm.

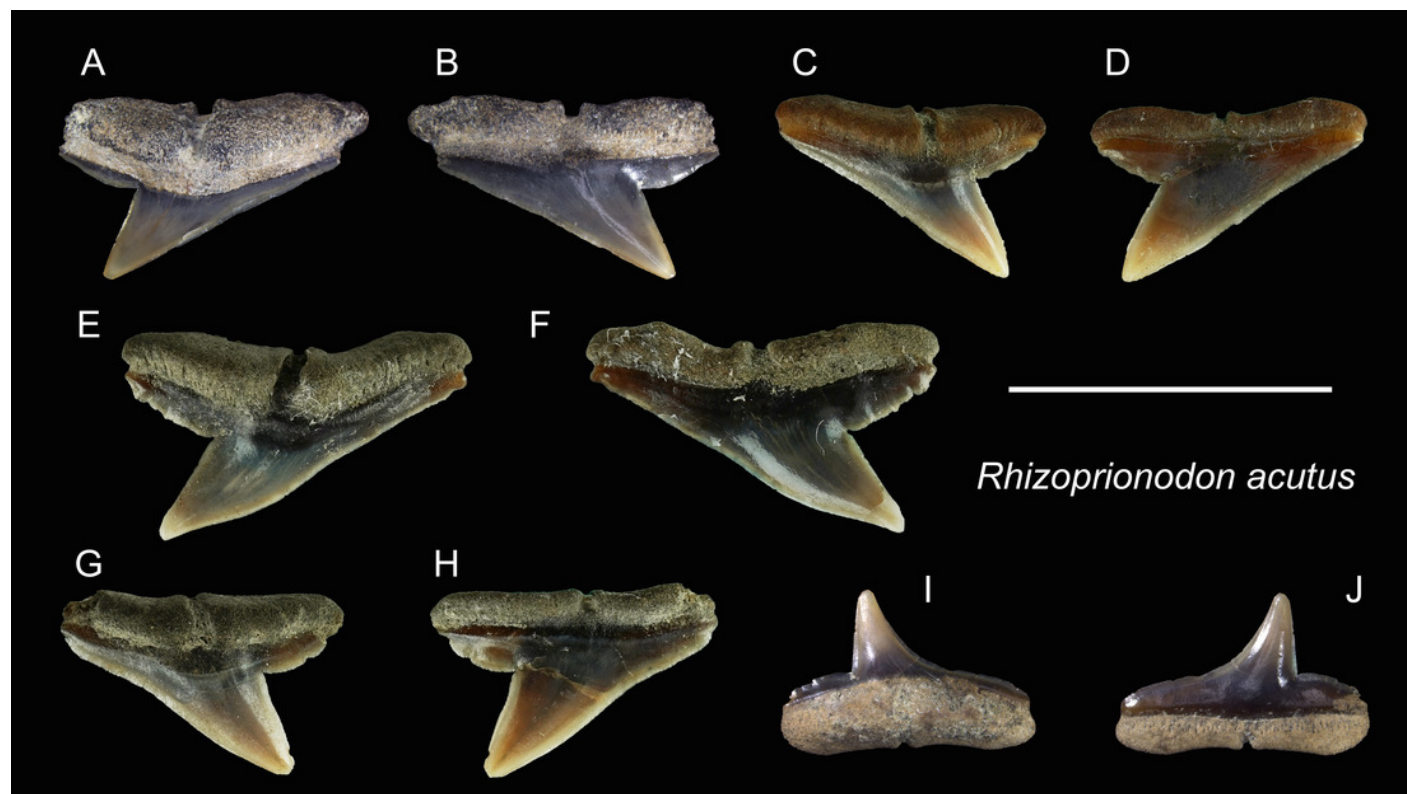


Figure 17

Teeth of *Galeocerdo cuvier* and *Sphyrna lewini* from the early Pleistocene of Liuchungchi Formation of Niubu, southern Taiwan.

A–H, *Galeocerdo cuvier*; A, B, CMM F0245; C, D, E, CMM F0215; F, G, H, ASIZF0100459. I–L, *Sphyrna lewini*; I, J, CMM F0235; K, L, CMM F0312. A, C, F, I, K = lingual views; B, D, G, J, L = labial views; E, H = details of secondary serrations. Scale bars = 1 cm.

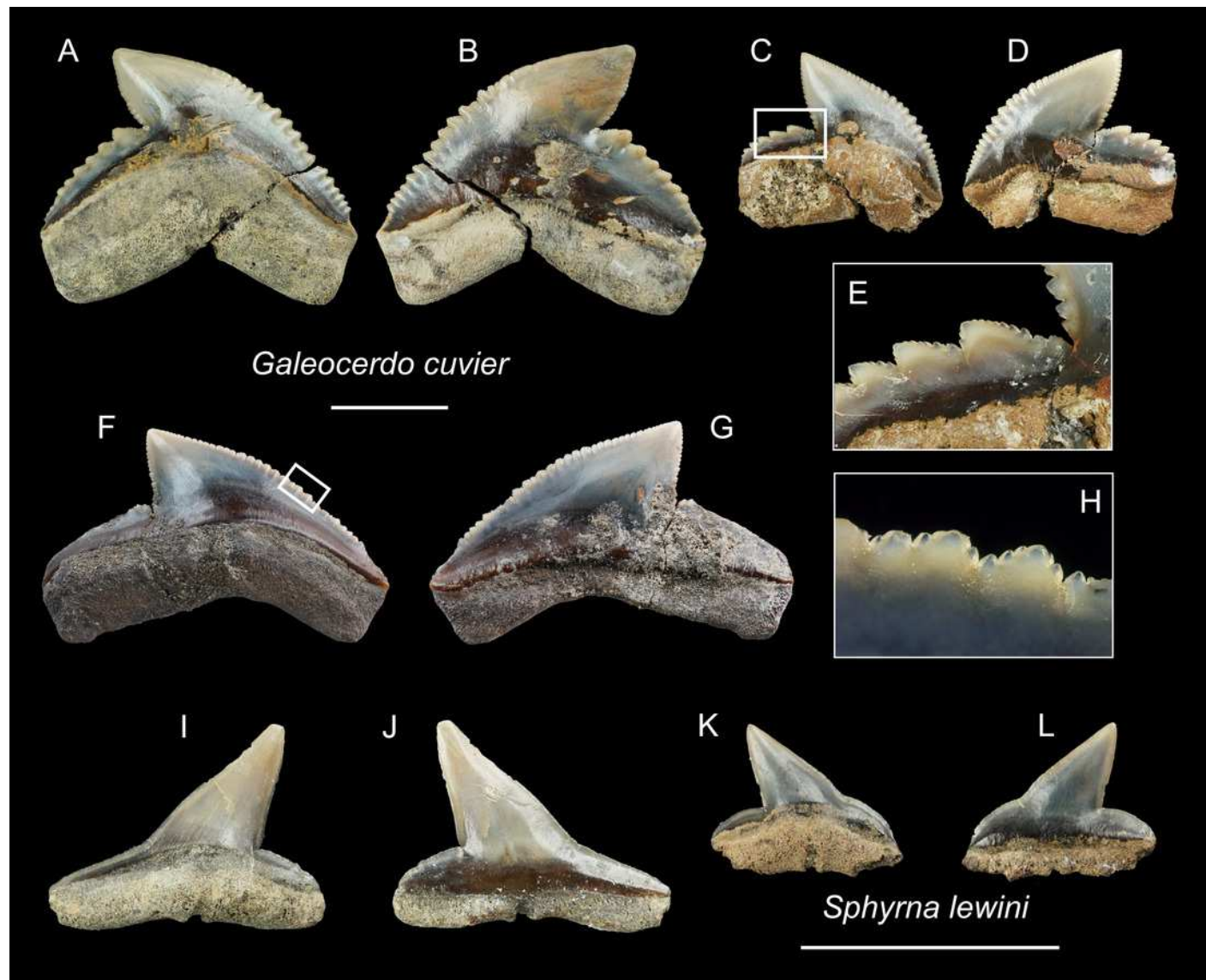


Figure 18

Teeth of Dasyatidae indet. from the early Pleistocene of Liuchungchi Formation of Niubu, southern Taiwan.

A, B, C, D, ASIZF0100590; E, F, G, H, ASIZF0100591. A, E = labial views; B, F = basal views; C, G = occlusal views; D, H = lateral views. Scale bar = 5 mm.

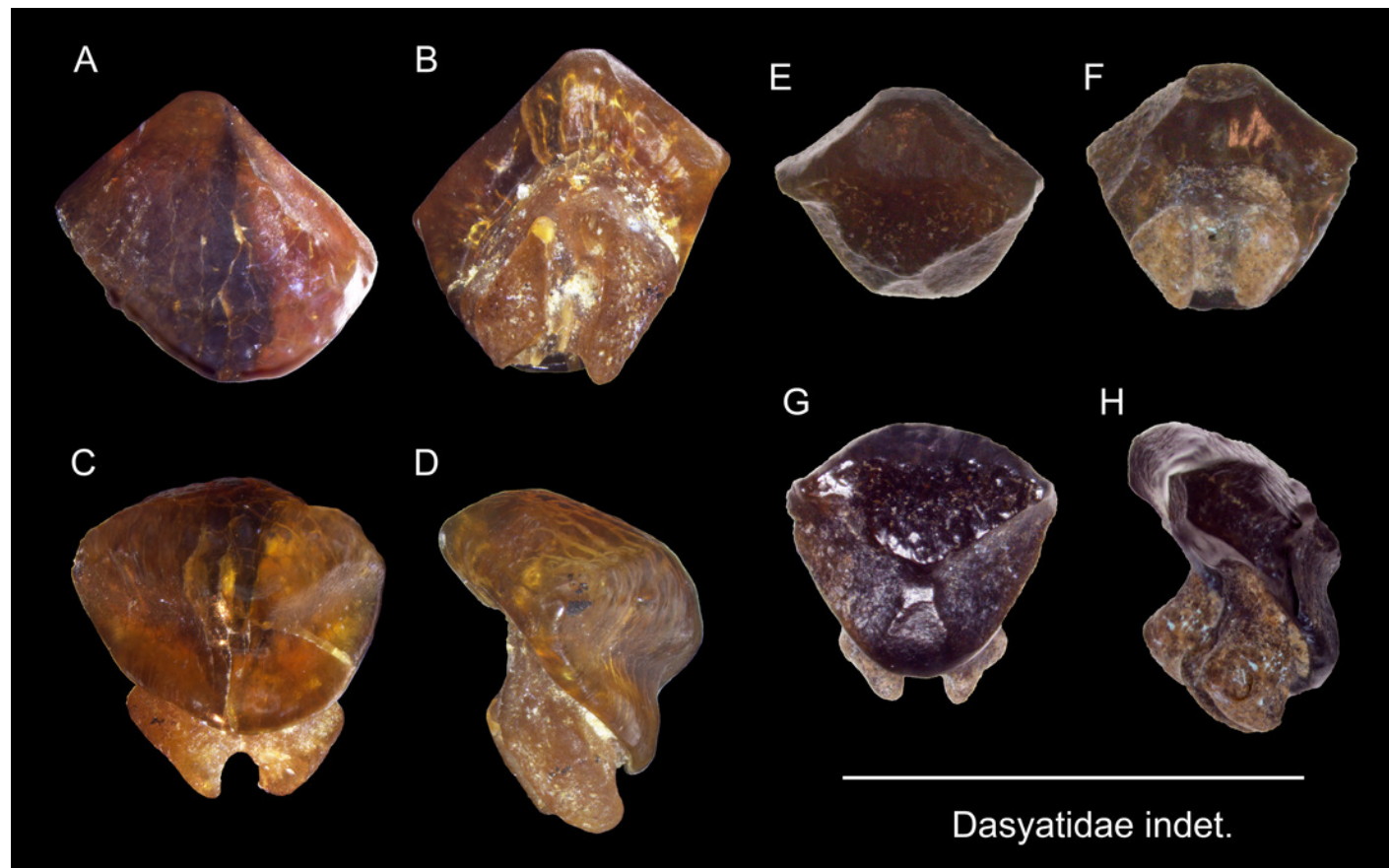


Figure 19

Teeth of *Aetobatus* sp. from the early Pleistocene of Liuchungchi Formation of Niubu, southern Taiwan.

A, B, CMM F2854; C, D, CMM F2850; E, F, CMM F0408; G, H, ASIZF0100549. A, C, E, G = occlusal views; B, D, F, H = basal views. Scale bar = 1 cm.

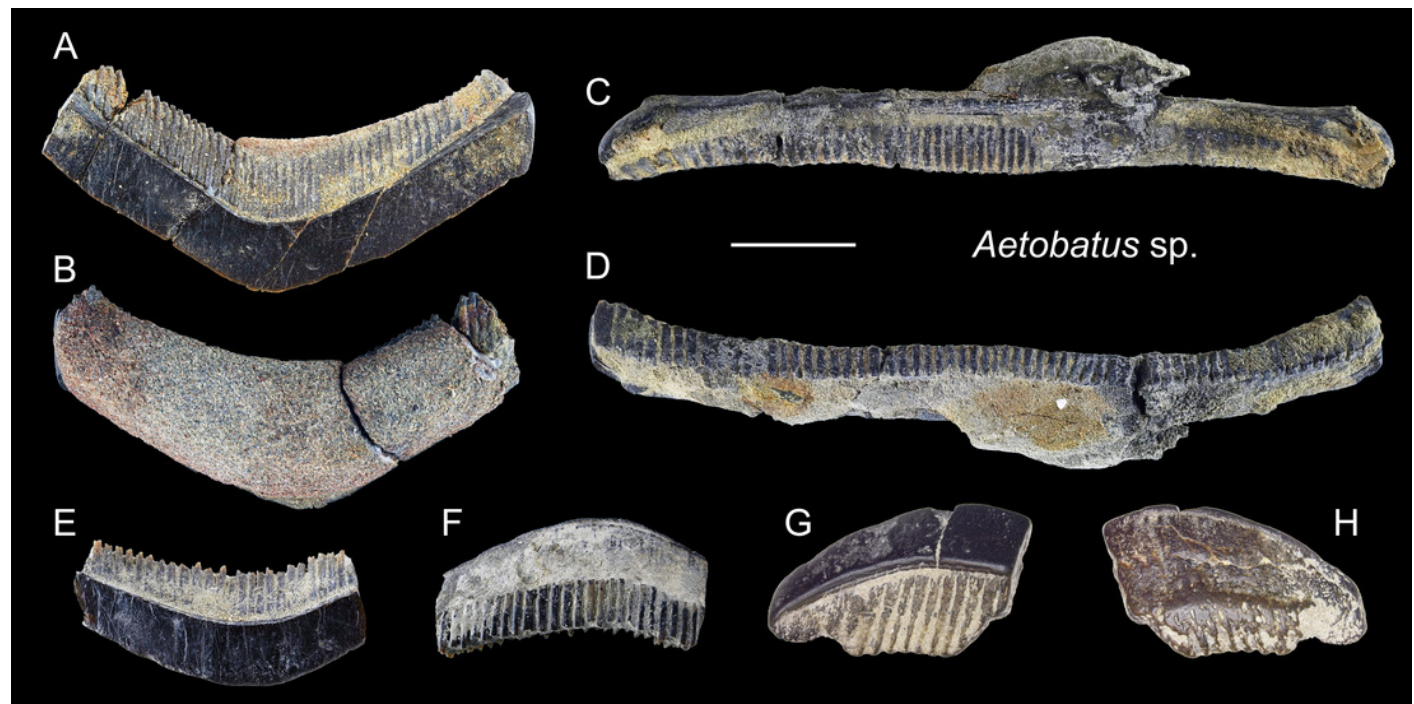


Figure 20

Teeth of *Myliobatis* sp. from the early Pleistocene of Liuchungchi Formation of Niubu, southern Taiwan.

A, B, C, D, ASIZF0100582; E, F, G, H, ASIZF0100587; I, J, K, L, ASIZF0100586; M, N, CMM F0395; O, P, CMM F2855; Q, R, CMM F0393; S, T, CMM F0398. A, E, I, M, O, Q, S = occlusal views; B, F, J, N, P, R, T = basal views; C, G, K = lingual views; D, H, L = labial views. Scale bars = 1 cm.

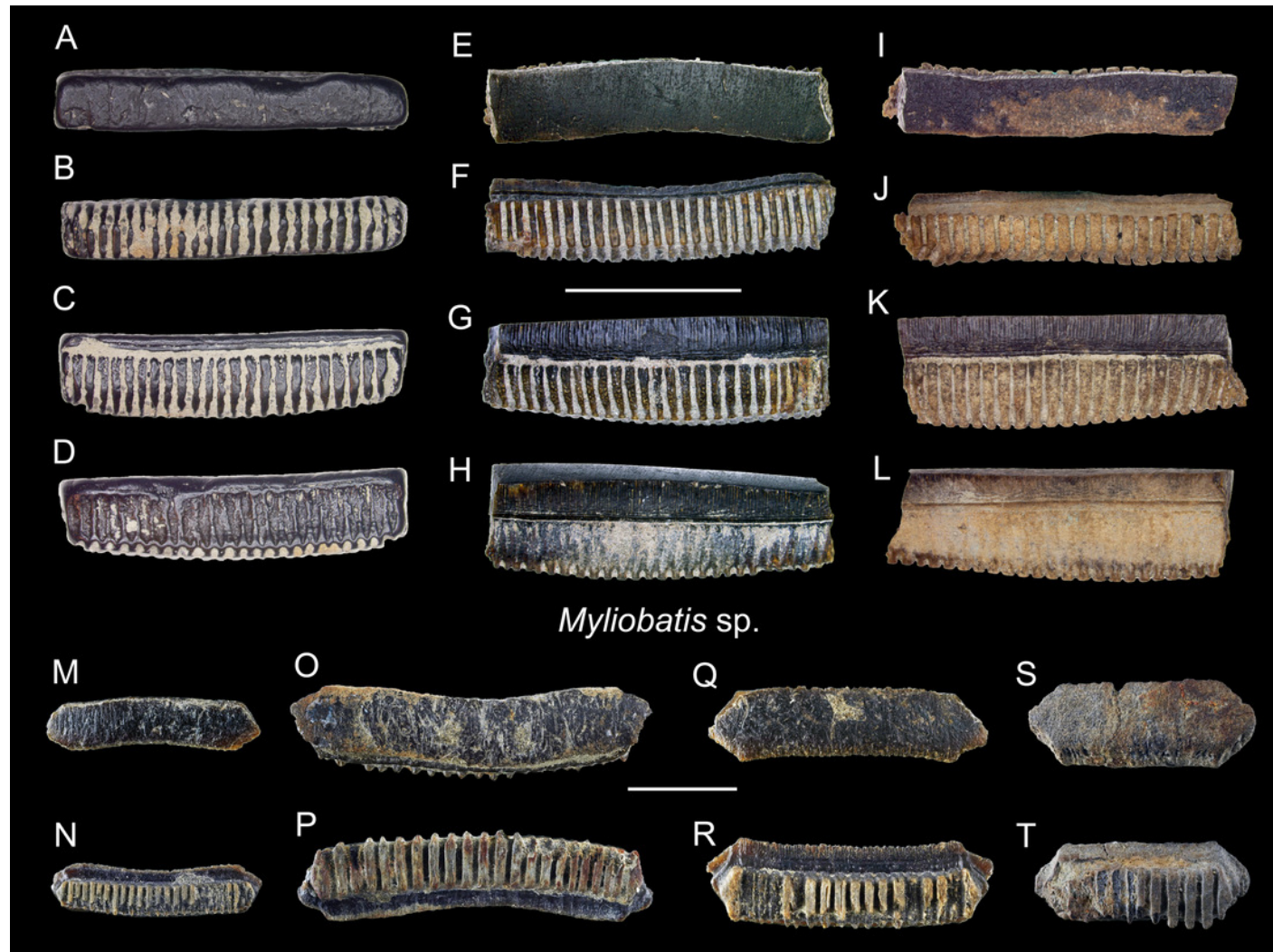


Table 1(on next page)

Elasmobranchs from the early Pleistocene Liuchungchi Formation of Niubu, southern Taiwan.

1 Table 1. Elasmobranchs from the early Pleistocene Liuchungchi Formation of Niubu, southern Taiwan.

2

Order	Family	Taxa	ASIZF	CMM	NTM	Total
Lamniformes	Carchariidae	<i>Carcharias taurus</i>	1	1		2
Lamniformes	Lamnidae	<i>Carcharodon carcharias</i>	28	25	2	55
Lamniformes	Lamnidae	<i>Isurus oxyrinchus</i>	4	1	1	6
Carcharhiniformes	Hemigaleidae	† <i>Hemipristis serra</i>	3	3	1	7
Carcharhiniformes	Carcharhinidae	<i>Carcharhinus altimus</i>	5	10	2	17
Carcharhiniformes	Carcharhinidae	<i>Carcharhinus amboinensis</i>	3	2		5
Carcharhiniformes	Carcharhinidae	<i>Carcharhinus leucas</i>	17	53	1	71
Carcharhiniformes	Carcharhinidae	<i>Carcharhinus limbatus</i>	16	21	3	40
Carcharhiniformes	Carcharhinidae	<i>Carcharhinus longimanus</i>	18	16	2	36
Carcharhiniformes	Carcharhinidae	<i>Carcharhinus obscurus</i>	9	15	1	25
Carcharhiniformes	Carcharhinidae	<i>Carcharhinus plumbeus</i>	8	42	1	51
Carcharhiniformes	Carcharhinidae	<i>Carcharhinus sorrah</i>	1	10		11
Carcharhiniformes	Carcharhinidae	<i>Carcharhinus tjtjot</i>	5	14		19
Carcharhiniformes	Carcharhinidae	<i>Carcharhinus</i> spp.	88	110	10	208
Carcharhiniformes	Carcharhinidae	<i>Rhizoprionodon acutus</i>	2	6		8
Carcharhiniformes	Galeocerdonidae	<i>Galeocerdo cuvier</i>	1	5	1	7
Carcharhiniformes	Sphyrnidae	<i>Sphyrna lewini</i>		2		2
Myliobatiformes	Dasyatidae	Dasyatidae indet.	2			2
Myliobatiformes	Aetobatidae	<i>Aetobatus</i> sp.	32	22	4	58
Myliobatiformes	Myliobatidae	<i>Myliobatis</i> sp.	9	20	1	30
Indet.	Indet.	Indet.	25	12		37
Total			277	390	30	697

3

Table 2(on next page)

Various diversity indices from the Pleistocene West Pacific elasmobranch assemblages showing high diversity of the present material.

See Supplemental Table S1 for details of the data.

1 Table 2. Various diversity indices from the Pleistocene West Pacific elasmobranch assemblages showing high diversity of the present
2 material. See Supplemental Table S1 for details of the data.

Location	Age	Species richness	Shannon	Simpson	Fisher's alpha	Reference
Taiwan	early Pleistocene	20	2.4	0.9	3.9	Our study
Sulawesi	Pleistocene	6	1.6	0.8	2.0	Hooijer, 1954
Java	Pleistocene	4	0.9	0.5	1.4	Koumans, 1949
Java	Plio-Pleistocene	11	1.7	0.7	2.9	Yudha et al., 2018
Central Japan	early Pleistocene	2	0.5	0.3	1.2	Karasawa, 1989
Central Japan	middle Pleistocene	14	2.2	0.9	6.0	Kawase & Nishimatsu, 2016
Eastern Japan	Pleistocene	14	2.3	0.9	4.6	Tanaka & Taru, 2022